Supplementary Information (SI) for Environmental Science: Processes & Impacts.


*Supporting information for*

# A 50-year record for perfluoroalkyl acids in the High Arctic: Implications for global and local transport

Daniel Persaud[1], Alison S. Criscitiello[2], Christine Spencer[3], Igor Lehnherr[4], Derek C G. Muir[3], Amila O. De Silva[3], and Cora J. Young[1].

[1]*Department of Chemistry, York University, Toronto, ON*

[2]*Department of Earth and Atmospheric Sciences, University of Alberta, Edmonton, Alberta, Canada.*

[3]*Aquatic Contaminants Research Division, Environmental and Climate Change Canada, Burlington, Ontario, Canada.*

[4]*Department of Geography, University of Toronto-Mississauga, Mississauga, Ontario, Canada.*

Correspondence: Cora J. Young (youngcj@yorku.ca) and Amila O. De Silva (amila.desilva@ec.gc.ca)

## 1.0 Method

### 1.1 Per- and polyfluoroalkyl substances (PFAS) analyzed in the current study

**Table S1:** Acronym, number of carbons, name/structure, and CAS No. of PFASs considered in this study.

| Acronym | Number of carbons | Name / Structure | CAS. No |
|---|---|---|---|
| **1. Perfluoroalkyl carboxylic acids (PFCAs)** | | | |
| PFPeA | 5 | perfluoropentanoic acid | 2706-90-3 |
| PFHxA | 6 | perfluorohexanoic acid | 307-24-4 |
| PFHpA | 7 | perfluorohepanoic acid | 375-85-9 |
| PFOA | 8 | perfluorooctanoic acid | 335-67-1 |
| PFNA | 9 | perfluorononanoic acid | 375-95-1 |
| PFDA | 10 | perfluorodecanoic acid | 335-76-2 |
| PFUnDA | 11 | perfluoroundecanoic acid | 2058-94-8 |
| PFDoDA | 12 | perfluorododecanoic acid | 307-55-1 |
| PFTrDA | 13 | perfluorotridecanoic acid | 72629-94-8 |
| PFTeDA | 14 | perfluorotetradecanoic acid | 376-06-7 |
| **2. Perfluoroalkyl sulfonic acids (PFSAs)** | | | |
| PFBS | 4 | perfluorobutane sulfonic acid | 375-73-5 |
| PFHxS | 6 | perfluorohexane sulfonic acid | 355-46-4 |
| PFHpS | 7 | Perfluoroheptane sulfonic acid | |
| PFOS | 8 | perfluorooctane sulfonic acid | 1763-23-1 |
| PFDS | 10 | Perfluorodecance sulfonic acid | 335-77-3 |
| PFECHS | 8 | perfluoroethylcyclohexane sulfonate | 646-83-3 |
| **3. Perfluorooctane sulfonamides/amidoethanols (xFOSA/Es)** | | | |
| FOSA | 8 | $C_8F_{17}SO_2NH_2$ | 754-91-6 |
| **4. Emerging PFAS (per- and polyfluorinated ethers)** | | | |
| HFPO-DA | 6 | $C_6HF_{11}O_3$ | 13252-13-6 |
| ADONA | 7 | $CF_3OC_3F_6OCFHCF_2CO_2$- | |
| 8Cl-PFOS | 8 | $ClC_8F_{16}SO_3$- | |
| 9Cl-PF3ONS | 8 | $ClC_6F_{12}OC_2F_4SO_3$ | Component of F-53B |
| 11Cl-PF3OUdS | 10 | $ClC_8F_{16}OC_2F_4SO_3$ | Component of F-53B |

## 1.2 Sample collection


**Figure S1:** Polar stereographic map of the Arctic region showing Mt. Oxford icefield, Canada (red circle), Thule Air Base, Qaanaaq, Greenland (green circle), Canada Forces Station (CFS) Alert (Blue Circle) and the Devon Ice Cap (yellow circle).

### 1.3 Ice core dating and sectioning

Dating of the ice core collected from Mt. Oxford icefield was done using oxygen stable isotope records and other glaciochemical records measured in a co-located core that was drilled simultaneously within a few metres from the core in the current study. A Picarro cavity ring – down spectroscopy analyzer was utilized to determine the oxygen isotope composition, the precision of $\delta^{18}O$ of water samples is ≤ 0.1 %. Sample isotope ratios were standardized using three working standards calibrated against the IAEA standards VSMOW and SLAP. Final $\delta^{18}O$ values are on the VSMOW/SLAP scale. The $\delta^{18}O$ time series were used to establish age-depth relationships by matching the $\delta^{18}O$ core records with local summer and winter solstice dates (linearly interpolating between solstices).[1] Elemental, ion, and $H_2O_2$ analyses for both cores were performed on an ICP-MS.[2] Where $\delta^{18}O$ records were ambiguous, we additionally used the non-sea salt sulfur/sodium (nssS/Na) summer peak (indicative of summer solstice) as well as $H_2O_2$ to ascertain the annual $\delta^{18}O$ maxima. We counted annual peaks in the remaining major ionic species to validate and confirm the accuracy of the age assignment (e.g., Figure S2). Validation of the oxygen isotope-based dating was done using (in this order): nss-S, $Na^+$, $H_2O_2$, $Mg^{2+}$, $Cl^-$, and $Ca^{2+}$. Further confirmation of dating assignment was conducted using the Pb-enrichment time series wherein the 1979 spike in Pb enrichment was used as a tie-point. The total dating error for this method is ±1 year. The 16.5 m ice core was separated and packaged into 1 m sections for transport.

Depths corresponding to a calendar year were determined as described above, and the dates of each 1 m section were subsequently determined. To section the cores, we removed the samples from a -38°C storage freezer into a refrigerated vestibule (-10°C). We then removed each 1 m section from the packaging and placed the firn and ice pieces onto aluminum foil that was previously cleaned with methanol. Each section was separated into a calendar year and placed in a labelled pre-cleaned polyethylene bottle. Using the aluminium foil underneath the firn and ice pieces ensured minimal loss and easy transfer to the polypropylene bottles. Samples were kept frozen at -38°C until extraction and analysis.

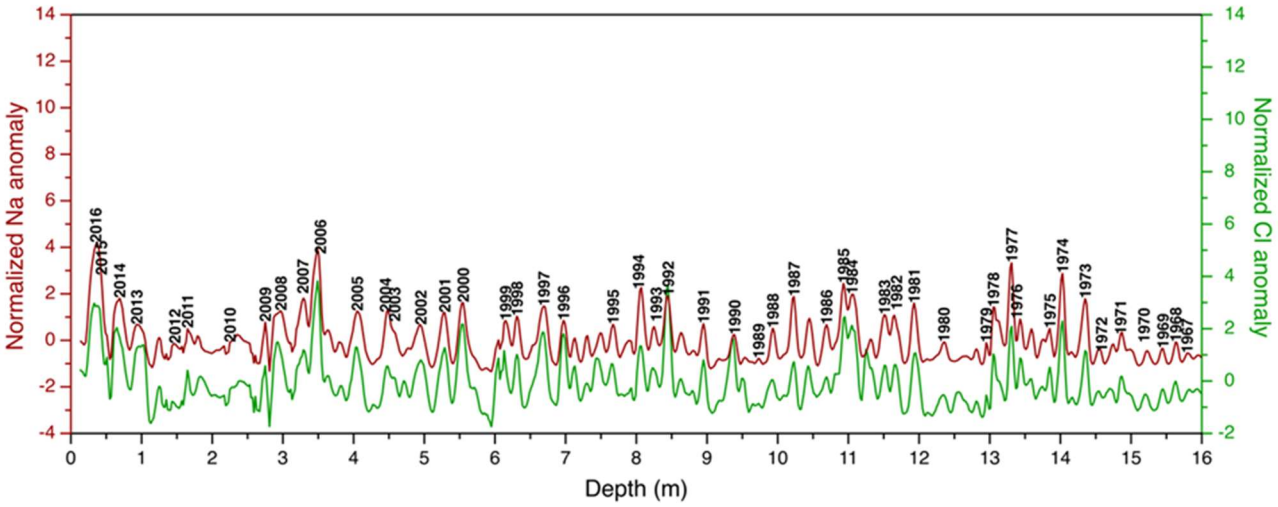


**Figure S2:** Sodium ($Na^+$) and chloride ($Cl^-$) ions measured in 2 cm intervals in an ice core collected on Mt Oxford icefield co-located with the ice core examined in this study. Na and Cl are expressed as normalized anomaly* with labels corresponding to the winter maxima year. Normalized anomaly = $\frac{(X-m)}{s}$, where X is the data point, $m\ and\ s$ are average and standard deviation, respectively. A three-point moving average smoother was also applied.

## 1.4 Controls for mitigating PFAS contamination in field sampling and lab processing

Extensive care was taken in handling the ice core to prevent contamination that could compromise the trace analysis of PFAAs. It is well established that PFAAs are extensively used in consumer applications; therefore, we specifically avoided products containing fluoropolymer coatings during the collecting, processing, and analysis of PFAAs. The ice core drill (Kovacs Mark II coring system, http://kovacsicedrillingequipment.com/coring-systems/mark-ii/) does not contain any material of concern which could potentially contaminate the ice core. It is also essential to note that the entire rind of the core was completely removed and discarded so that any firn or ice that was touching the inner circumference of the barrel is removed to mitigate contamination.

Additionally, we previously prepared field exposed blanks consisting of HPLC grade water that was transported to the field site, opened, and exposed to the atmosphere in the Arctic location Resolute Bay, Nunavut. These samples were shipped back to the lab, extracted, and analyzed with methods analogous to the ice core samples and compared to HPLC water stored in the lab (See Pickard et al., 2018 for further details).

The results from this exercise indicated that environmental exposure and shipping do not contribute to PFAS contamination. We acknowledge that these field banks have limitations and are not identical to an ice core.

Contamination was also minimized during sectioning and analysis. Extensive planning was done to ensure that the ice core was handled minimally to reduce the risk of contamination. Sectioning itself was done in a refrigerated vestibule that is only used for ice core sectioning and has controlled temperature, humidity airflow and pressure. Only one person handled the actual core, everyone in the room wore nitrile gloves and lab coats. The ice core was placed on a stainless-steel table that was lined with pre-cleaned heavy duty aluminum foil sheets. We used a stainless-steel saw that was cleaned with solvent between each annual layer. After each cut the foil was discarded. The ability to constrain contamination during ice core collection and handling is an important area for future studies.

### 1.5 PFAS chemical extraction and analysis

The sample extraction procedure was adapted from Pickard et al.[1] Prior to extraction, sub-samples were spiked with internal standards (IS) to monitor recovery and matrix effects. Additionally, before instrument analysis, sample extracts were spiked with instrument performance standards (IP) to account for matrix effects and instrument drift. Table S2 outlines the IS and IP standards used, the analyte ion transitions used are also included.

Chromatographic separation of targeted PFAS were separated using an Acquity UPLC BEH C18 column (Waters Acquity UPLC® BEH, 2.1 x 50 mm,1.7 µm) with a water – methanol gradient elution. An isolator column was employed to separate background contamination from the sample injection. The composition of the mobile phases was 98/2 SPE-cleaned water/methanol containing 2 mM ammonium acetate (A) and MeOH (B). All solvents were HPLC grade. The method was a fifteen-minute run, at a flow rate of 0.3 mL $min^{-1}$. A summary of the chromatographic conditions for this gradient method is shown in Table S3. The inlet and mass spectrometric conditions used for separation is summarized in Table S4.

**Table S2:** Analyte quantifier and qualifier ion transitions (m/z) and internal standards used for PFAAs analysis. Internal standards were used to evaluate recovery and matrix effects, whereas instrument performance standards were used to evaluate matrix effects only. Precursor ion/product ion transitions (m/z) are indicated in brackets.

| PFAAs | Quantifier/Qualifier Ion Transitions (m/z) | Internal Standards | Instrument Performance Standards |
|---|---|---|---|
| PFPeA | 263 > 219 | $^{13}C_5$ PFPeA (268/223) | $^{13}C_3$ PFPeA (266/222) |
| PFHxA | 313 > 269 / 313 > 119 | $^{13}C_2$ PFHxA (315/270) | $^{13}C_5$ PFHxA (318/273) |
| PFHpA | 363 > 319 / 363 > 169 | $^{13}C_4$ PFHpA (367/322) | |
| PFOA | 413 > 369 / 413 > 169 | $^{13}C_4$ PFOA (417/372) | $^{13}C_2$ PFOA (415/370) |
| PFNA | 463 > 419 / 463 > 219 | $^{13}C_5$ PFNA (468/423) | $^{13}C_9$ PFNA (472/427) |
| PFDA | 513 > 469 / 513 > 219 | $^{13}C_2$ PFDA (515/470) | $^{13}C_6$ PFDA (519/474) |
| PFUnDA | 563 > 519 / 563 > 269 | $^{13}C_2$ PFUnDA (565/520) | $^{13}C_7$ PFUnDA (570/525) |
| PFDoDA | 613 > 569 / 613 > 169 | $^{13}C_2$ PFDoDA (615/570) | |
| PFTrDA | 663 > 619 / 663 > 169 | $^{13}C_2$ PFDoDA (615/570) | |
| PFTeDA | 713 > 669 / 663 > 169 | $^{13}C_2$ PFTeDA (715/670) | |
| PFHxDA | 813 > 769 / 813 > 169 | $^{13}C_2$ PFHxDA (815/770) | |
| PFBS | 299 > 80 / 229 > 99 | $^{13}C_3$ PFBS (302/99) | |
| PFHxS | 399 > 80 / 399 > 99 | $^{18}O_2$ PFHxS (403/103) | $^{13}_{C3}$ PFHxS (402/99) |
| PFHpS | 449 > 80 / 449 > 99 | $^{18}O_2$ PFHxS (403/103) | |
| PFOS | 499 > 80 / 499 > 99 | $^{13}C_4$ PFOS (503/99) | $^{13}C_8$ PFOS (507/99) |
| PFDS | 599 > 80 / 599 > 99 | $^{13}C_4$ PFOS (503/99) | |
| FOSA | 498 > 78 | $^{13}C_8$ FOSA (506/78) | |
| PFECHS | 461 > 381 / 461 > 99 | $^{18}O_2$ PFHxS (403/103) | |
| HFPO-DA | 285>169 | MHFPO-DA (287/ 169) | |
| ADONA | 377>251, 377 > 85 | $^{18}O_2$ PFHxS (403/103) | |
| 8Cl-PFOS | 515 > 80, 517 > 80 | $^{13}C_4$ PFOS (503/99) | |
| 9Cl-PF3ONS | 531 > 83, 531 > 351 | $^{13}C_4$ PFOS (503/99) | |
| 11Cl-PF3OUdS | 631 > 83, 631 > 451 | $^{13}C_4$ PFOS (503/99) | |

**Table S3:** Summary of chromatographic conditions: A is 98/2 SPE-cleaned water/methanol containing 2 mM ammonium acetate and B is MeOH.

| Time (minutes) | Flow rate (mL $min^{-1}$) | % A | % B |
|---|---|---|---|
| 0 | 0.400 | 75 | 25 |
| 0.5 | 0.400 | 75 | 25 |
| 5.0 | 0.400 | 15 | 85 |
| 5.1 | 0.400 | 0 | 100 |
| 5.6 | 0.400 | 0 | 100 |
| 7.0 | 0.400 | 0 | 100 |
| 9.0 | 0.400 | 75 | 25 |
| 15.0 | 0.400 | 75 | 25 |

**Table S4:** Summary of inlet and mass spectrometric conditions.

| | |
|---|---|
| Capillary Voltage (kV) | 0.7 |
| Source Offset (V) | 50 |
| Source Temperature (°C) | 150 |
| Desolvation Gas Temperature (°C) | 450 |
| Cone Gas Flow (L $hr^{-1}$) | 150 |
| Desolvation Gas Flow (L $hr^{-1}$) | 800 |
| Collision Gas Flow (mL $min^{-1}$) | 0.15 |
| Nebulizer Pressure (bar) | 7.0 |
| Column Temperature (°C) | 50 |
| Injection Volume (µL) | 9.0 |

## 1.6 Major Ion Analysis in melted ice core section

Sub samples of the sectioned ice core (15 mL) were analyzed for major anions and cations. Cation analysis was done using a Dionex 6000 Ion chromatography system coupled to a conductivity detector. Separation was achieved using a Dionex IonPac CS19 (4 x 250 mm) column equipped with a guard column (Dionex IonPac GS19, 4 x 50 mm) using an isocratic elution method with methanesulfonic acid at 1.0 mL $min^{-1}$. The eluent was supressed (CRDS 600 ion suppressor, 4 mm) before the analytes were measured. Calibration standards were prepared by serial dilution from the stock standard (Dionex 6 Cation I standard). In addition to calibration standards, two check standards and reagent blank were run every ten (10) samples.

## 1.7 Quality Control and Quality Assurance

The mean recoveries and standard errors for the IS and IP standards are provided in Tables S5 and S6. Recoveries are based on peak area comparisons to spiked solvent standards. The accuracy was evaluated by spiking an Arctic freshwater composite matrix (n=2) with native standards (final concentration in extract is 3 ng/mL) and treating analogous to a sample (see Table S7). To obtain the composite matrix, excess melted sample from each discrete layer was combined. The final concentrations were then compared to the theoretical spiked concentrations. Similarly, two additional 500 mL aliquots were taken through the extraction method but only spiked with isotopically labeled standards just prior to the instrumental analysis (post extraction spikes).

**Table S5:** Recovery of IS in sample extracts. Standards with number refers to the different ion transitions (m/z). Recovery is based on peak area in sample extracts compared to spiked solvent standard. Mean (standard deviation) recovery reported for n = 50 samples from the Mt. Oxford icefield.

| Internal Standards | Recovery (%) |
|---|---|
| $^{13}C_5$ PFPeA | 63 (7.1) |
| $^{13}C_2$ PFHxA | 64 (6.6) |
| $^{13}C_4$ PFHpA | 69 (5.9) |
| $^{13}C_4$ PFOA | 71 (5.6) |
| $^{13}C_5$ PFNA | 72 (5.6) |
| $^{13}C_2$ PFDA | 67 (8.9) |
| $^{13}C_2$ PFUnDA | 57 (14) |
| $^{13}C_2$ PFDoDA | 43 (14) |
| $^{13}C_2$ PFTeDA | 56 (21) |
| $^{13}C_2$ PFHxDA | 121 (60) |
| $^{13}$C8 FOSA | |
| $^{13}C_4$ PFOS | 70(6.2) |
| $^{18}O_2$ PFHxS | 76 (4.3) |
| $^{13}C_3$ PFBS | 76 (4.4) |
| $^{13}C_3$ HFPO-DA | 72 (6.7) |

**Table S6:** Recovery of isotopically labeled instrument performance (IP) standards in sample extracts. Recovery based on peak area in sample extract divided by peak area in spiked calibration standard at the same concentration. Mean (standard deviation) recovery reported for n = 50 samples from the Mt. Oxford icefield.

| Instrument Performance Standards | Recovery (%) |
|---|---|
| $^{13}C_3$ PFPeA | 86 (6.2) |
| $^{13}C_5$ PFHxA | 82 (5.0) |
| $^{13}C_2$ PFOA | 84 (6.0) |
| $^{13}C_9$ PFNA | 85 (6.5) |
| $^{13}C_6$ PFDA | 88 (6.2) |
| $^{13}C_7$ PFUnDA | 88 (7.2) |
| $^{13}C_8$ PFOS 80 | 84 (5.6) |
| $^{13}C_8$ PFOS 99 | 84 (5.5) |

**Table S7:** Calculated recoveries of Native PFAS analytes in spiked Arctic freshwater composite samples. Two samples were spiked before extraction and two samples were spiked after extraction. The range in calculated recovery is presented.

| PFAAs | Recovery in sample spiked before extraction (%), n=2 | Recovery in sample spiked after extraction (%), n=2 |
|---|---|---|
| PFPeA | 99-104 | 97-100 |
| PFHxA | 94-100 | 88-99 |
| PFHpA | 96-101 | 97-98 |
| PFOA | 78-90 | 78-81 |
| PFNA | 95-97 | 93-94 |
| PFDA | 99-103 | 92-100 |
| PFUnDA | 96-106 | 98-102 |
| PFDoDA | 97-103 | 92-97 |
| PFTrDA | 70-85 | 99-108 |
| PFTeDA | 102-113 | 98-100 |
| PFHxDA | 113-115 | 100-101 |
| PFBS | | |
| PFHxS | 95-105 | 96-99 |
| PFHpS | 101-106 | 95-99 |
| PFOS | 87-95 | 94-102 |
| PFDS | 68-87 | 94-96 |
| FOSA | 96-103 | 100-100 |
| PFECHS | 92-101 | 93-97 |
| HFPO-DA | 95-103 | 94-95 |
| ADONA | 113-119 | 112-117 |
| 8Cl-PFOS | 100-106 | 102-102 |
| 9Cl-PF3ONS | 88-98 | 92-98 |
| 11Cl-PF3OUdS | NA | NA |

Cartridge blanks (n=8) were included in the method analysis. Briefly, SPE conditioned water was spiked with the internal standard, extracted, and treated analogously as a sample. In addition, regular injections of MeOH and 1:1 MeOH/water were injected during the instrument batch to evaluate lab contamination and carryover. The method detection limit (MDL) is based on the average raw signal in method blanks plus 3 times the standard deviation. This concentration was transformed into sample units by multiplying by the final extract volume of 0.5 ml and dividing by a theoretical sample volume of 0.5 L to obtain units relatable to sample reporting. The instrument detection limit was estimated using the IUPAC method, based on analysis of low-level calibration standards (near blank with signal to noise of less than 10) and the slope of the calibration curve (*m*):

$$\mathrm{LOD} = \frac{\mathrm{k}\,S_B}{\mathrm{m}}$$

Where $S_B$ is the standard deviation of the raw signal in low level calibration standards and k = 3.

**Table S8:** Instrument detection limit (LOD, ng/mL) based on calibration standard with S/N of 3 and method detection limit (MDL, ng/L) based on average + 3 times standard deviation of method blanks. Method detection limit is in units comparable to sample concentrations.

| Internal Standards | LOD (ng/mL) | MDL (ng/L) |
|---|---|---|
| PFPeA | 0.0032 | 0.0098 |
| PFHxA | 0.0120 | 0.0390 |
| PFHpA | 0.0039 | 0.0074 |
| PFOA | 0.0061 | 0.0130 |
| PFNA | 0.0054 | 0.0037 |
| PFDA | 0.0022 | 0.0045 |
| PFUnDA | 0.0099 | 0.0051 |
| PFDoDA | 0.0044 | 0.0025 |
| PFTrDA | 0.0014 | 0.0050 |
| PFTeDA | 0.0120 | 0.0075 |
| PFHxDA | 0.0590 | 0.0960 |
| PFBS | 0.0056 | 0.0080 |
| PFHxS | 0.0048 | 0.0074 |
| PFHpS | 0.0042 | 0.0055 |
| PFOS | 0.0081 | 0.0760 |
| PFDS | 0.0110 | 0.0034 |
| PFECHS | 0.0028 | 0.0330 |
| FOSA | 0.0010 | 0.0041 |
| HFPO-DA | 0.0360 | 0.0120 |
| 8Cl PFOS | 0.0059 | 0.0032 |
| ADONA | 0.0063 | 0.0010 |
| 9Cl-PF3ONS | 0.0102 | 0.0045 |
| 11Cl-PF3OUdS | 0.0053 | 0.0028 |

## 1.8 Data Handling

### Correlation Analysis

Correlation analysis was conducted on fluxes of PFAAs and major ions in ice sections. Only detected values were included (i.e., <LOD were excluded). The annual fluxes of PFAA and ions were logarithm-transformed [$\log_{10}$ PFAA,ions] to approximate normality, which was evaluated using Shapiro-Wilk tests of kurtosis and skewness. Significant correlations using Pearson correlation coefficient (r) was based on threshold of $p<0.05$. In addition, correlations were classified as very strong (0.90-1.0), strong (0.70-0.90), moderate (0.50-0.70) and weak (0.30-0.50).

### Calculating Deposition Flux

Fluxes for each analyte were calculated for each calendar year. The analyte concentration (ng/L) was multiplied by the total ice volume per year (L/yr) and divided by the area ($m^2$).

$$\text{Flux} = \frac{\text{Analyte Concentration } \left(\frac{\text{ng}}{\text{L}}\right) \text{ x Total ice volume per year } \left(\frac{\text{L}}{\text{yr}}\right)}{\text{Area } (\text{m}^2)}$$

(Area = $\pi r^2$, where r = 3.85 cm)

## 1.9 Air Mass Transport Densities

Air mass back-trajectories were calculated to help characterize the probable marine moisture source regions and flow pathways of air masses reaching the ice core site. Annual air parcel back trajectories were calculated using the NOAA Hybrid Single-Particle Lagrangian Integrated Trajectory (HySPLIT) model.[3] HySPLIT has been used previously to assess the transport pathways of precipitation to Arctic ice core sites (e.g., Criscitiello et al., 2016; Criscitiello et al., 2021).[4,5] Ten-day back trajectories were calculated using National Centers for Environmental Protection and Atmospheric Research (NCEP/NCAR) global atmospheric reanalysis data sets, with a focus on low-elevation air masses (0–500 m above terrain) that are more likely to be representative of evaporation moisture sources.[6] We subsequently calculated air mass transport densities from single trajectories to derive more reliable airflow pathways and help discriminate between local circulation patterns and regional-scale flow features.[5,7] The air mass transport density results are discussed in the context of ice core chemistry, and offer insight into probable airflow pathways arriving at the ice core site during time periods of interest in this study.

## 2.0 PFAA Concentration and Fluxes at the Mt. Oxford icefield

**Table S9**: Depth profile (cm) of long chain PFCAs concentrations (ng $L^{-1}$) from Mt. Oxford icefield. Values <MDL are identified in red.

| | | Concentration (ng $L^{-1}$) | | | | | | | |
|---|---|---|---|---|---|---|---|---|---|
| **Depth(cm)** | **Year** | **PFPeA** | **PFHxA** | **PFHpA** | **PFOA** | **PFNA** | **PFDA** | **PFUnDA** | **PFDoDA** |
| 41 | 2016 | 0.254 | 0.465 | 0.951 | 0.857 | 1.147 | 0.118 | 0.084 | 0.011 |
| 63 | 2015 | 0.218 | 0.386 | 0.574 | 0.546 | 0.806 | 0.095 | 0.057 | 0.007 |
| 89 | 2014 | 0.280 | 0.509 | 0.882 | 0.976 | 1.147 | 0.113 | 0.087 | 0.014 |
| 138 | 2013 | 0.121 | 0.245 | 0.439 | 0.635 | 1.113 | 0.140 | 0.203 | 0.016 |
| 163 | 2012 | 0.104 | 0.288 | 0.533 | 0.862 | 2.330 | 0.191 | 0.276 | 0.025 |
| 191 | 2011 | 0.104 | 0.168 | 0.255 | 0.484 | 0.488 | 0.058 | 0.034 | <0.0025 |
| 227 | 2010 | 0.230 | 0.422 | 0.324 | 0.530 | 0.745 | 0.159 | 0.119 | 0.020 |
| 279 | 2009 | 0.141 | 0.205 | 0.348 | 0.346 | 0.510 | 0.110 | 0.122 | 0.017 |
| 325 | 2008 | 0.279 | 0.420 | 0.526 | 0.651 | 0.778 | 0.109 | 0.093 | 0.012 |
| 353 | 2007 | 0.140 | 0.281 | 0.457 | 0.754 | 0.730 | 0.078 | 0.072 | 0.011 |
| 399 | 2006 | 0.186 | 0.390 | 0.539 | 0.905 | 0.949 | 0.106 | 0.090 | 0.014 |
| 413 | 2005 | 0.220 | 0.370 | 0.607 | 0.887 | 0.982 | 0.136 | 0.118 | 0.016 |
| 447 | 2004 | 0.118 | 0.165 | 0.257 | 0.434 | 0.543 | 0.078 | 0.092 | 0.018 |
| 490 | 2003 | 0.136 | 0.191 | 0.323 | 0.525 | 0.638 | 0.054 | 0.027 | 0.004 |
| 517 | 2002 | 0.137 | 0.208 | 0.368 | 0.552 | 0.677 | 0.123 | 0.099 | 0.012 |
| 545 | 2001 | 0.090 | 0.153 | 0.296 | 0.429 | 0.462 | 0.059 | 0.014 | 0.003 |
| 587 | 2000 | 0.123 | 0.218 | 0.316 | 0.464 | 0.589 | 0.086 | 0.081 | 0.016 |
| 615 | 1999 | 0.142 | 0.220 | 0.368 | 0.417 | 0.652 | 0.104 | 0.091 | 0.013 |
| 661 | 1998 | 0.115 | 0.228 | 0.333 | 0.391 | 0.386 | 0.064 | 0.051 | <0.0025 |
| 687 | 1997 | 0.119 | <0.0390 | <0.0074 | <0.0130 | <0.0037 | <0.0045 | <0.0051 | <0.0025 |
| 733 | 1996 | 0.102 | 0.234 | 0.377 | 0.404 | 0.583 | 0.081 | 0.060 | 0.011 |
| 775 | 1995 | 0.084 | 0.193 | 0.240 | 0.376 | 0.294 | 0.039 | 0.031 | 0.008 |
| 809 | 1994 | 0.058 | 0.165 | 0.160 | 0.282 | 0.218 | 0.034 | 0.027 | <0.0025 |
| 835 | 1993 | 0.042 | 0.132 | 0.137 | 0.248 | 0.167 | 0.025 | 0.021 | <0.0025 |
| 878 | 1992 | 0.048 | 0.111 | 0.130 | 0.268 | 0.158 | 0.026 | 0.013 | <0.0025 |
| 920 | 1991 | 0.057 | 0.183 | 0.167 | 0.486 | 0.228 | 0.039 | 0.014 | <0.0025 |
| 971 | 1990 | 0.037 | 0.091 | 0.078 | 0.263 | 0.071 | 0.015 | 0.006 | <0.0025 |
| 987 | 1989 | 0.021 | 0.092 | 0.053 | 0.098 | 0.042 | 0.030 | 0.005 | <0.0025 |
| 1010 | 1988 | 0.012 | 0.085 | 0.050 | 0.100 | 0.061 | 0.020 | 0.009 | 0.005 |
| 1057 | 1987 | <0.0098 | 0.030 | 0.036 | 0.076 | 0.036 | 0.018 | 0.007 | <0.0025 |
| 1079 | 1986 | 0.013 | 0.036 | 0.031 | 0.070 | 0.032 | 0.025 | 0.005 | <0.0025 |
| 1103 | 1985 | 0.011 | 0.051 | 0.045 | 0.155 | 0.046 | 0.019 | 0.002 | <0.0025 |
| 1138 | 1984 | 0.011 | 0.049 | 0.037 | 0.132 | 0.033 | 0.019 | 0.005 | 0.004 |
| 1172 | 1983 | 0.013 | 0.034 | 0.022 | 0.071 | 0.012 | 0.013 | 0.002 | <0.0025 |
| 1190 | 1982 | 0.015 | 0.034 | 0.021 | 0.058 | 0.012 | 0.014 | 0.004 | 0.004 |
| 1233 | 1981 | 0.020 | 0.028 | 0.017 | 0.042 | 0.010 | 0.011 | 0.004 | 0.008 |
| 1277 | 1980 | 0.066 | 0.012 | 0.017 | 0.041 | 0.007 | 0.010 | 0.002 | <0.0025 |
| 1300 | 1979 | 0.012 | 0.678 | 0.060 | 0.054 | 0.011 | 0.018 | <0.0051 | 0.006 |
| 1318 | 1978 | 0.004 | 0.206 | 0.012 | 0.061 | 0.010 | 0.009 | <0.0051 | <0.0025 |
| 1332 | 1977 | 0.025 | 0.016 | 0.011 | 0.036 | 0.008 | 0.009 | <0.0051 | <0.0025 |
| 1363 | 1976 | 0.029 | 0.010 | 0.006 | 0.048 | 0.007 | 0.014 | <0.0051 | 0.001 |
| 1389 | 1975 | 0.041 | 0.020 | 0.011 | 0.044 | 0.012 | 0.018 | 0.005 | 0.002 |
| 1410 | 1974 | 0.013 | 0.067 | 0.034 | 0.652 | 0.076 | 0.040 | 0.040 | 0.016 |
| 1438 | 1973 | 0.016 | 0.063 | 0.045 | 1.078 | 0.096 | 0.038 | 0.013 | 0.006 |
| 1461 | 1972 | <0.0098 | 0.009 | 0.006 | 0.039 | 0.011 | 0.013 | 0.002 | 0.003 |
| 1482 | 1971 | 0.035 | 0.016 | 0.007 | 0.084 | 0.009 | 0.018 | 0.003 | 0.002 |
| 1515 | 1970 | 0.035 | 0.003 | 0.006 | 0.069 | 0.018 | 0.010 | 0.003 | 0.004 |
| 1547 | 1969 | <0.0098 | 0.022 | 0.012 | 0.136 | 0.018 | 0.014 | 0.003 | <0.0025 |
| 1575 | 1968 | <0.0098 | 0.016 | 0.010 | 0.053 | 0.006 | 0.012 | 0.002 | 0.004 |
| 1588 | 1967 | <0.0098 | 0.030 | 0.010 | 0.121 | 0.011 | 0.006 | <0.0051 | <0.0025 |

**Table S10:** Depth profile (cm) of PFSA concentrations (ng $L^{-1}$) from Mt. Oxford icefield. Values <MDL are identified in red.

| | | Concentration (ng $L^{-1}$) | | | |
|---|---|---|---|---|---|
| **Depth(cm)** | **Year** | **PFBS** | **PFOS** | **PFECHS** | **FOSA** |
| 41 | 2016 | 0.037 | 0.267 | 0.065 | 0.008 |
| 63 | 2015 | 0.046 | 0.264 | 0.094 | 0.004 |
| 89 | 2014 | 0.008 | 0.025 | 0.011 | 0.008 |
| 138 | 2013 | 0.007 | 0.026 | 0.040 | 0.005 |
| 163 | 2012 | 0.021 | 0.074 | 0.045 | 0.009 |
| 191 | 2011 | 0.005 | 0.032 | 0.033 | 0.011 |
| 227 | 2010 | 0.015 | 0.071 | 0.067 | 0.009 |
| 279 | 2009 | 0.006 | 0.021 | 0.116 | 0.004 |
| 325 | 2008 | 0.017 | 0.082 | 0.117 | 0.012 |
| 353 | 2007 | 0.005 | 0.038 | 0.050 | 0.037 |
| 399 | 2006 | 0.007 | 0.048 | 0.020 | 0.059 |
| 413 | 2005 | 0.070 | 0.476 | 0.077 | 0.050 |
| 447 | 2004 | 0.005 | <0.0760 | 0.048 | 0.044 |
| 490 | 2003 | 0.004 | <0.0760 | <0.0330 | 0.035 |
| 517 | 2002 | 0.021 | 0.001 | 0.011 | 0.064 |
| 545 | 2001 | 0.002 | <0.0760 | <0.0330 | 0.065 |
| 587 | 2000 | 0.029 | 0.213 | 0.053 | 0.059 |
| 615 | 1999 | 0.008 | 0.050 | 0.021 | 0.064 |
| 661 | 1998 | 0.017 | 0.087 | 0.029 | 0.056 |
| 687 | 1997 | <0.0080 | <0.0760 | <0.0330 | 0.037 |
| 733 | 1996 | 0.008 | 0.079 | 0.065 | 0.041 |
| 775 | 1995 | 0.008 | 0.054 | 0.022 | 0.032 |
| 809 | 1994 | 0.007 | 0.029 | 0.027 | 0.030 |
| 835 | 1993 | 0.017 | 0.144 | 0.048 | 0.027 |
| 878 | 1992 | 0.015 | 0.114 | 0.104 | 0.028 |
| 920 | 1991 | 0.006 | 0.041 | 0.019 | 0.017 |
| 971 | 1990 | 0.004 | 0.006 | 0.039 | 0.004 |
| 987 | 1989 | 0.434 | 4.168 | 0.065 | 0.007 |
| 1010 | 1988 | 0.017 | 0.116 | 0.083 | 0.011 |
| 1057 | 1987 | 0.006 | 0.019 | 0.067 | 0.004 |
| 1079 | 1986 | 0.015 | 0.037 | 0.018 | 0.008 |
| 1103 | 1985 | 0.067 | 0.452 | 0.040 | 0.008 |
| 1138 | 1984 | 0.019 | 0.104 | 0.075 | 0.009 |
| 1172 | 1983 | 0.022 | 0.130 | 0.082 | 0.004 |
| 1190 | 1982 | 0.012 | 0.099 | 0.062 | 0.003 |
| 1233 | 1981 | 0.005 | 0.023 | 0.061 | <0.0041 |
| 1277 | 1980 | 0.004 | 0.014 | 0.142 | <0.0041 |
| 1300 | 1979 | 0.687 | 1.355 | 0.090 | 0.002 |
| 1318 | 1978 | 0.011 | 0.035 | 0.033 | 0.002 |
| 1332 | 1977 | 0.012 | 0.086 | 0.022 | 0.002 |
| 1363 | 1976 | 0.076 | 1.235 | 0.030 | 0.002 |
| 1389 | 1975 | 0.017 | 0.022 | 0.132 | <0.0041 |
| 1410 | 1974 | 0.014 | 0.090 | 0.098 | <0.0041 |
| 1438 | 1973 | 0.014 | 0.153 | 0.122 | <0.0041 |
| 1461 | 1972 | 0.002 | <0.0760 | 0.043 | <0.0041 |
| 1482 | 1971 | 0.007 | 0.012 | 0.064 | <0.0041 |
| 1515 | 1970 | 0.112 | 1.654 | 0.023 | <0.0041 |
| 1547 | 1969 | 0.022 | 0.157 | 0.046 | <0.0041 |
| 1575 | 1968 | 0.009 | 0.033 | 0.032 | <0.0041 |
| 1588 | 1967 | 0.009 | 0.081 | 0.064 | <0.0041 |

**Table S11:** Depth profile (cm) of PFCA fluxes (ng $m^2$ $a^{-1}$) on the Mt Oxford icefield. Numbers in red indicate instances where ½ MDL was used for annual flux calculation.

| | | Flux (ng $m^2$ $a^{-1}$) | | | | | | | |
|---|---|---|---|---|---|---|---|---|---|
| **Depth(cm)** | **Year** | **PFPeA** | **PFHxA** | **PFHpA** | **PFOA** | **PFNA** | **PFDA** | **PFUnDA** | **PFDoDA** |
| 41 | 2016 | 37.27 | 68.24 | 139.56 | 125.76 | 168.32 | 17.32 | 12.33 | 1.61 |
| 63 | 2015 | 16.98 | 30.06 | 44.70 | 42.52 | 62.76 | 7.40 | 4.44 | 0.55 |
| 89 | 2014 | 34.00 | 61.82 | 107.12 | 118.53 | 139.30 | 13.72 | 10.57 | 1.70 |
| 138 | 2013 | 34.38 | 69.62 | 124.75 | 180.44 | 316.27 | 39.78 | 57.68 | 4.55 |
| 163 | 2012 | 9.87 | 27.32 | 50.56 | 81.77 | 221.03 | 18.12 | 26.18 | 2.37 |
| 191 | 2011 | 37.15 | 60.02 | 91.10 | 172.90 | 174.33 | 20.72 | 12.15 | 0.45 |
| 227 | 2010 | 21.03 | 38.59 | 29.63 | 48.47 | 68.13 | 14.54 | 10.88 | 1.83 |
| 279 | 2009 | 50.29 | 73.12 | 124.13 | 123.42 | 181.92 | 39.24 | 43.52 | 6.06 |
| 325 | 2008 | 64.29 | 96.78 | 121.20 | 150.01 | 179.27 | 25.12 | 21.43 | 2.77 |
| 353 | 2007 | 17.56 | 35.25 | 57.34 | 94.60 | 91.59 | 9.79 | 9.03 | 1.38 |
| 399 | 2006 | 43.52 | 91.26 | 126.12 | 211.76 | 222.06 | 24.80 | 21.06 | 3.28 |
| 413 | 2005 | 12.94 | 21.77 | 35.71 | 52.18 | 57.77 | 8.00 | 6.94 | 0.94 |
| 447 | 2004 | 18.93 | 26.47 | 41.24 | 69.64 | 87.13 | 12.52 | 14.76 | 2.89 |
| 490 | 2003 | 32.16 | 45.17 | 76.39 | 124.16 | 150.89 | 12.77 | 6.39 | 0.95 |
| 517 | 2002 | 22.51 | 34.18 | 60.48 | 90.71 | 111.26 | 20.21 | 16.27 | 1.97 |
| 545 | 2001 | 12.74 | 21.66 | 41.90 | 60.73 | 65.40 | 8.35 | 1.98 | 0.42 |
| 587 | 2000 | 26.99 | 47.84 | 69.35 | 101.83 | 129.27 | 18.87 | 17.78 | 3.51 |
| 615 | 1999 | 21.52 | 33.35 | 55.78 | 63.21 | 98.83 | 15.76 | 13.79 | 1.97 |
| 661 | 1998 | 30.27 | 60.01 | 87.65 | 102.91 | 101.60 | 16.85 | 13.42 | 0.33 |
| 687 | 1997 | 17.97 | 2.94 | 5.59 | 0.98 | 0.28 | 0.34 | 0.39 | 0.19 |
| 733 | 1996 | 26.41 | 60.59 | 97.62 | 104.61 | 150.96 | 20.97 | 15.54 | 2.85 |
| 775 | 1995 | 22.18 | 50.96 | 63.38 | 99.29 | 77.63 | 10.30 | 8.19 | 2.11 |
| 809 | 1994 | 12.13 | 34.51 | 33.47 | 58.99 | 45.60 | 7.11 | 5.65 | 0.26 |
| 835 | 1993 | 7.46 | 23.46 | 24.35 | 44.07 | 29.68 | 4.44 | 3.73 | 0.22 |
| 878 | 1992 | 12.78 | 29.55 | 34.61 | 71.35 | 42.07 | 6.92 | 3.46 | 0.33 |
| 920 | 1991 | 15.83 | 50.81 | 46.37 | 134.93 | 63.30 | 10.83 | 3.89 | 0.35 |
| 971 | 1990 | 11.99 | 29.49 | 25.27 | 85.22 | 23.01 | 4.86 | 1.94 | 0.41 |
| 987 | 1989 | 2.30 | 10.09 | 5.81 | 10.75 | 4.61 | 3.29 | 0.55 | 0.14 |
| 1010 | 1988 | 1.98 | 14.02 | 8.25 | 16.50 | 10.06 | 3.30 | 1.48 | 0.82 |
| 1057 | 1987 | 1.54 | 9.43 | 11.32 | 23.90 | 11.32 | 5.66 | 2.20 | 0.39 |
| 1079 | 1986 | 1.95 | 5.41 | 4.66 | 10.52 | 4.81 | 3.76 | 0.75 | 0.19 |
| 1103 | 1985 | 1.72 | 7.97 | 7.03 | 24.22 | 7.19 | 2.97 | 0.31 | 0.20 |
| 1138 | 1984 | 2.73 | 12.18 | 9.20 | 32.81 | 8.20 | 4.72 | 1.24 | 0.99 |
| 1172 | 1983 | 3.62 | 9.46 | 6.12 | 19.75 | 3.34 | 3.62 | 0.56 | 0.35 |
| 1190 | 1982 | 2.40 | 5.43 | 3.36 | 9.27 | 1.92 | 2.24 | 0.64 | 0.64 |
| 1233 | 1981 | 7.46 | 10.44 | 6.34 | 15.66 | 3.73 | 4.10 | 1.49 | 2.98 |
| 1277 | 1980 | 20.54 | 3.74 | 5.29 | 12.76 | 2.18 | 3.11 | 0.62 | 0.39 |
| 1300 | 1979 | 2.07 | 116.69 | 10.33 | 9.29 | 1.89 | 3.10 | 0.44 | 1.03 |
| 1318 | 1978 | 0.53 | 27.51 | 1.60 | 8.15 | 1.34 | 1.20 | 0.34 | 0.17 |
| 1332 | 1977 | 2.67 | 1.71 | 1.17 | 3.84 | 0.85 | 0.96 | 0.27 | 0.13 |
| 1363 | 1976 | 7.16 | 2.47 | 1.48 | 11.85 | 1.73 | 3.46 | 0.63 | 0.25 |
| 1389 | 1975 | 8.16 | 3.98 | 2.19 | 8.75 | 2.39 | 3.58 | 0.99 | 0.40 |
| 1410 | 1974 | 2.15 | 11.06 | 5.61 | 107.65 | 12.55 | 6.60 | 6.60 | 2.64 |
| 1438 | 1973 | 3.30 | 13.00 | 9.28 | 222.39 | 19.80 | 7.84 | 2.68 | 1.24 |
| 1461 | 1972 | 0.82 | 1.51 | 1.01 | 6.55 | 1.85 | 2.18 | 0.34 | 0.50 |
| 1482 | 1971 | 5.57 | 2.55 | 1.11 | 13.37 | 1.43 | 2.86 | 0.48 | 0.32 |
| 1515 | 1970 | 9.98 | 0.86 | 1.71 | 19.68 | 5.13 | 2.85 | 0.86 | 1.14 |
| 1547 | 1969 | 1.17 | 5.26 | 2.87 | 32.50 | 4.30 | 3.35 | 0.72 | 0.30 |
| 1575 | 1968 | 1.16 | 3.77 | 2.36 | 12.49 | 1.41 | 2.83 | 0.47 | 0.94 |
| 1588 | 1967 | 0.54 | 3.32 | 1.11 | 13.40 | 1.22 | 0.66 | 0.28 | 0.14 |

**Table S12:** Depth profile (cm) of PFSA fluxes (ng $m^2$ $a^{-1}$) on the Mt Oxford icefield. Numbers in red indicate instances where ½ MDL was used for annual flux calculation.

| Depth(cm) | Year | PFBS | PFOS | PFECHS | FOSA |
|---|---|---|---|---|---|
| 41 | 2016 | 5.42 | 39.24 | 9.53 | 1.17 |
| 63 | 2015 | 3.56 | 20.59 | 7.29 | 0.35 |
| 89 | 2014 | 0.96 | 3.08 | 1.34 | 1.00 |
| 138 | 2013 | 2.06 | 7.36 | 11.27 | 1.48 |
| 163 | 2012 | 2.03 | 7.03 | 4.30 | 0.89 |
| 191 | 2011 | 1.94 | 11.43 | 11.72 | 3.84 |
| 227 | 2010 | 1.36 | 6.53 | 6.13 | 0.79 |
| 279 | 2009 | 2.18 | 7.43 | 41.24 | 1.46 |
| 325 | 2008 | 3.81 | 18.81 | 27.00 | 2.74 |
| 353 | 2007 | 0.67 | 4.73 | 6.26 | 4.62 |
| 399 | 2006 | 1.57 | 11.14 | 4.61 | 13.89 |
| 413 | 2005 | 4.12 | 28.02 | 4.54 | 2.96 |
| 447 | 2004 | 0.78 | 6.10 | 7.73 | 7.05 |
| 490 | 2003 | 0.94 | 8.99 | 3.90 | 8.24 |
| 517 | 2002 | 3.38 | 0.24 | 1.73 | 10.44 |
| 545 | 2001 | 0.21 | 5.38 | 2.34 | 9.24 |
| 587 | 2000 | 6.35 | 46.82 | 11.68 | 12.97 |
| 615 | 1999 | 1.27 | 7.65 | 3.23 | 9.63 |
| 661 | 1998 | 4.44 | 22.85 | 7.57 | 14.82 |
| 687 | 1997 | 0.60 | 5.74 | 2.49 | 5.66 |
| 733 | 1996 | 2.16 | 20.50 | 16.80 | 10.72 |
| 775 | 1995 | 2.00 | 14.24 | 5.73 | 8.36 |
| 809 | 1994 | 1.41 | 6.00 | 5.58 | 6.34 |
| 835 | 1993 | 2.96 | 25.52 | 8.51 | 4.79 |
| 878 | 1992 | 3.92 | 30.28 | 27.80 | 7.32 |
| 920 | 1991 | 1.65 | 11.39 | 5.35 | 4.63 |
| 971 | 1990 | 1.34 | 1.85 | 12.67 | 1.36 |
| 987 | 1989 | 47.57 | 457.11 | 7.13 | 0.79 |
| 1010 | 1988 | 2.86 | 19.19 | 13.63 | 1.79 |
| 1057 | 1987 | 1.79 | 5.86 | 21.07 | 1.30 |
| 1079 | 1986 | 2.32 | 5.57 | 2.66 | 1.19 |
| 1103 | 1985 | 10.54 | 70.61 | 6.24 | 1.23 |
| 1138 | 1984 | 4.66 | 25.85 | 18.65 | 2.18 |
| 1172 | 1983 | 6.10 | 36.26 | 22.76 | 1.11 |
| 1190 | 1982 | 1.93 | 15.75 | 9.95 | 0.47 |
| 1233 | 1981 | 1.80 | 8.59 | 22.89 | 0.73 |
| 1277 | 1980 | 1.13 | 4.20 | 44.05 | 0.64 |
| 1300 | 1979 | 118.27 | 233.24 | 15.55 | 0.34 |
| 1318 | 1978 | 1.40 | 4.69 | 4.45 | 0.27 |
| 1332 | 1977 | 1.24 | 9.16 | 2.31 | 0.22 |
| 1363 | 1976 | 18.79 | 304.80 | 7.48 | 0.48 |
| 1389 | 1975 | 3.37 | 4.36 | 26.34 | 0.41 |
| 1410 | 1974 | 2.32 | 14.90 | 16.18 | 0.34 |
| 1438 | 1973 | 2.81 | 31.49 | 25.22 | 0.42 |
| 1461 | 1972 | 0.34 | 6.38 | 7.18 | 0.34 |
| 1482 | 1971 | 1.11 | 1.83 | 10.22 | 0.33 |
| 1515 | 1970 | 31.83 | 471.64 | 6.66 | 0.58 |
| 1547 | 1969 | 5.29 | 37.53 | 11.06 | 0.71 |
| 1575 | 1968 | 2.04 | 7.75 | 7.58 | 0.23 |
| 1588 | 1967 | 1.03 | 8.97 | 7.11 | 0.11 |

**Table S13:** PFAA fluxes (ng $m^2$ $a^{-1}$) comparisions with other selected Arctic, sub-Arctic, and lower latitude samples.

| | | Flux (ng $m^2$ $a^{-1}$) | | | | | | | | | |
|---|---|---|---|---|---|---|---|---|---|---|---|
| **Matrix (Time)** | **Site (Reference)** | **PFPeA** | **PFHxA** | **PFHpA** | **PFOA** | **PFNA** | **PFDA** | **PFUnDA** | **PFDoDA** | **PFBS** | **PFOS** |
| Ice Core (1967-2016) | Mt. Oxford icefield, Canadian Arctic (this study) | 0.5 - 64 | 0.8 - 117 | 1 - 139 | 3.8 - 222 | 0.8 - 316 | 0.6 - 40 | 0.3 - 60 | 0.3 - 6 | 0.2 - 118 | 0.2 - 472 |
| Ice Core (2006-2019) | Lomonsovfonna Ice Core, Svalbard | 41-570 | 8 - 120 | 5 - 99 | 3 - 59 | 4 - 120 | 2 - 47 | 1-79 | 0.4 - 16 | | 0.22- 70 |
| Ice Core (1977-2015) | Devon Ice Cap, Canadian Arctic [8] | 1 - 37 | 3 - 38 | 6 - 86 | 6 - 80.50 | 5 - 141 | 0.5 - 21 | 0.8 – 29 | 0.2 - 2 | 0.7 – 0.9 | 1 - 80 |
| Snow Pit 1995 – 2007 | Devon Ice Cap, Canadian Arctic [9] | 7 – 68 | 5 – 60 | 21 - 99 | 25 – 97 | 25 – 219 | 9 - 35 | 4 – 38 | 0.1 – 4 | 14 - 42 | 1 – 4 |
| Snow Pit 1966 – 2006 | Devon Ice Cap, Canadian Arctic [10] | 2.5 – 9 | | | 21 – 81 | 2 – 103 | 1 – 9 | 1 – 10 | | | 1 – 28 |
| Surface Snow 2005 | Melville Ice Cap, Canadian Arctic[10] | | | | 5 | 3 | 1 | | | | |
| Surface Snow 2005 | Agassiz Ice Cap, Canadian Arctic[10] | | | | 4 | 3 | 1 | | | | |
| Snow Core 1980 - 2010 | Mt. Muztagata, Tibetan Plateau [11] | 20 - 90 | 7 - 63 | | 15 – 154 | 3 – 26 | 2 – 32 | 2 - 6 | 4 - 21 | | 208 - 195 |
| Snow Core 1980 – 2010 | Mt. Zuoqiupu, Tibetan Plateau [11] | 32 - 46 | 6 – 45 | | 27 – 188 | 2 – 22 | 30 – 56 | | | | |
| Firn Core 1996 - 2008 | Colle Gnifetti, Swiss/Italian Border [12] | | | | 165 - 207 | 86 - 113 | | 0 - 53 | | | |
| Precipitation (2006-2007 & 2007-2008) [a] | Ksukuba, Japan [13] | 686 | 1143 | 814 | 1955 | 2120 | 551 | 508 | 121 | | 475 |
| Precipitation (2006-2007 & 2007-2008)[a] | Kawaguchi, Japan[13] | 817 | 1185 | 983.5 | 2475 | 2270 | 425 | 534 | 86 | 5880 | 1133 |
| Precipitation (2006-2007) | Slingerlands, NY, US[13] | 219 | 834 | 627 | 2050 | 2070 | 243 | 456 | 37 | 8 | 401 |
| Precipitation (2006-2007) [b] | Downtown Albany, NY, US[13] | 857 | 1050 | 534 | 2090 | 2032 | 297 | 794 | 5 | | 255 |
| Precipitation (1998-1999) [b] | Rural U.S. (Ithaca, New York)[14] | 129 | 113 | 66 | 143 | 33 | | | | | |
| Precipitation 2002 [b] | Remote Canada (Kejimkujik, NS)[14] | 9 | 6 | 16 | 12 | 12 | | | | | |
| Precipitation (2003-2004)[b] | Urban Canada (Toronto, ON)[14] | 38 | 30 | 60 | 169 | 17 | | | | | |

## 3.0 PFAA deposition and temporal variations

The integrity of temporal trends could be affected by post-depositional processes, such as melting, percolation and refreezing. The propensity of PFAAs to percolate downwards during snowmelt depends on several factors including the specific snow surface area, PFAA chain length, and sorptive capacity of the snow grain surface.[15] Laboratory studies suggest that short chain PFAAs have a greater tendency to partition into meltwater whereas long chain compounds will sorb to snow surface or experience delayed release.[15,16]

If melting occurred within the last five decades, we expect the seasonal trends of PFAA deposition could be distorted but the annual interpretations should not be affected since any meltwater that percolates downward should refreeze within an interannual layer.[17] To circumvent errors associated with sectioning, dating and post depositional processes, we report fluxes as five year moving averages, which allows for a multidecadal temporal trend analysis of PFAS deposition to Mt Oxford icefield.

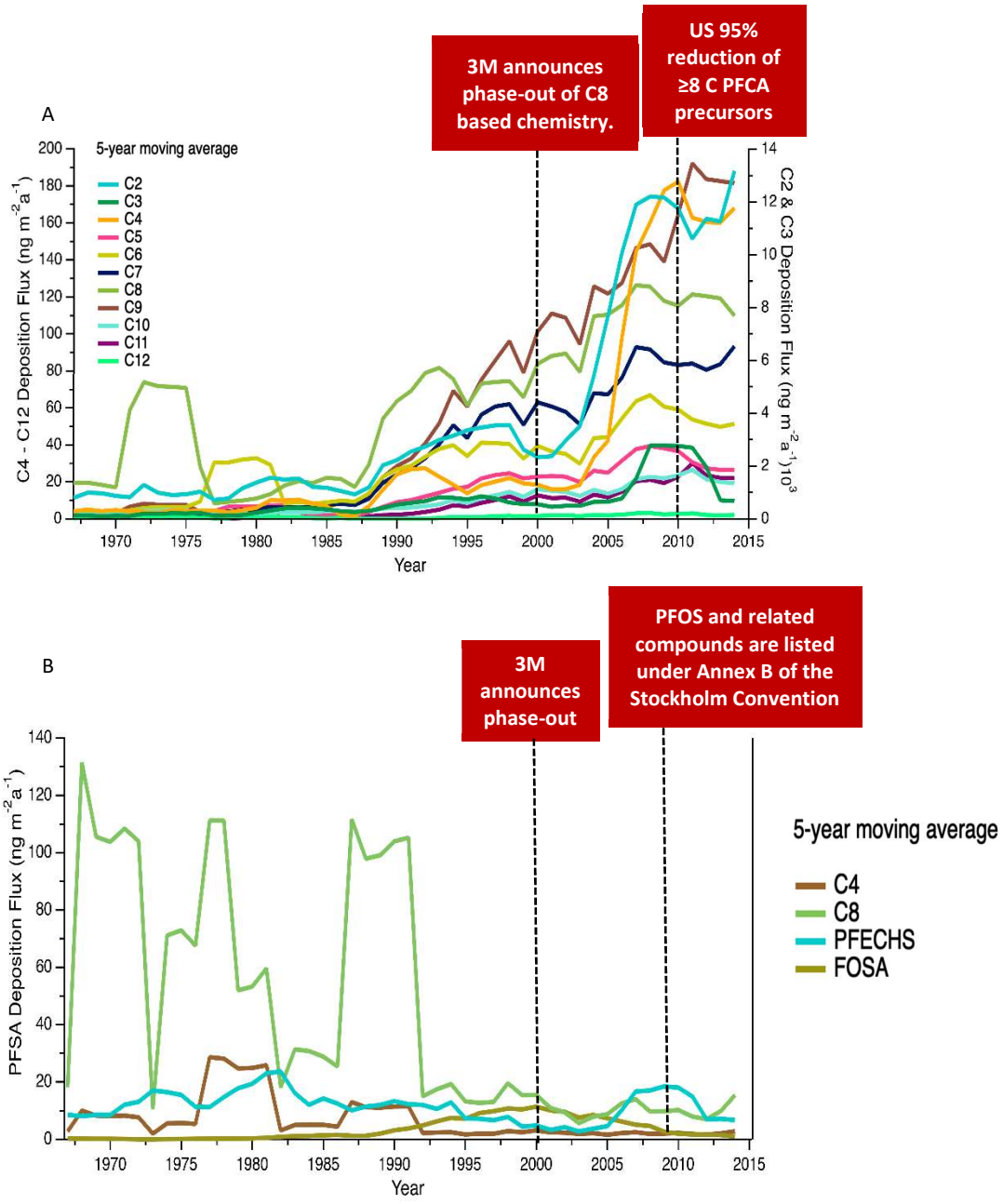


**Figure S3:** Five year moving averages of (A) C2– C12 PFCA and (B) C4 PFSA, C8 PFSA, PFECHS and FOSA deposition fluxes on Mt. Oxford icefield for the entire sampling period. Regulatory and major industry changes are also included.

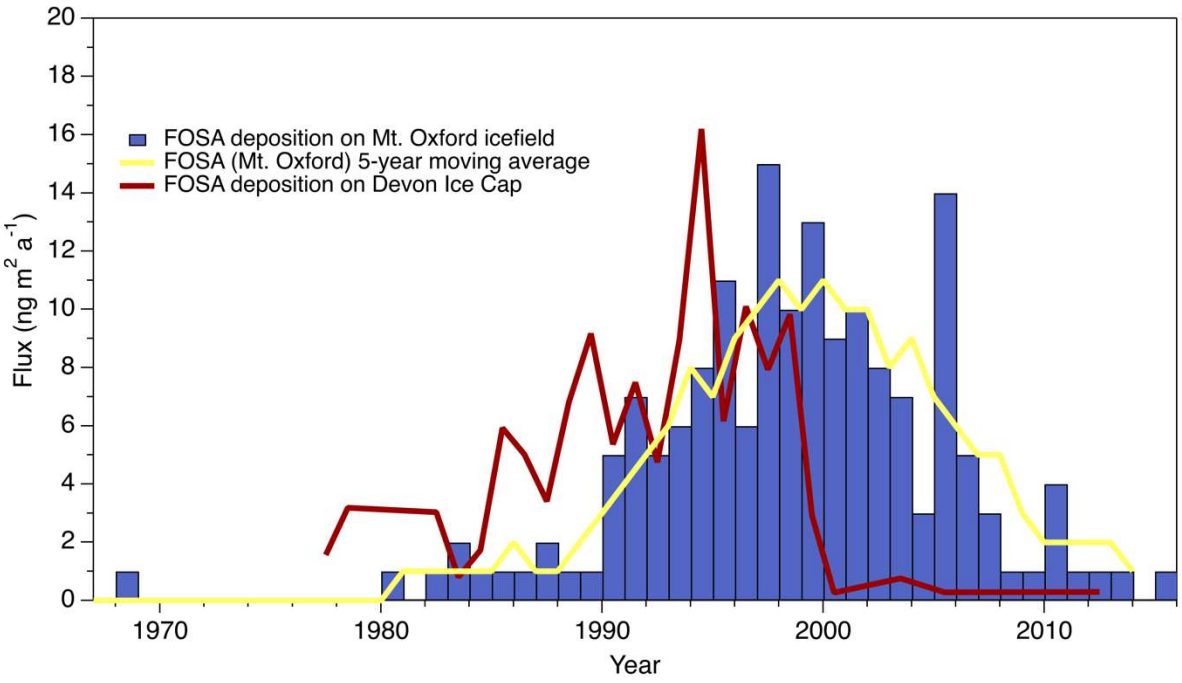


**Figure S4**: FOSA fluxes (ng $m^2$ $a^{-1}$) at Mt. Oxford icefield annual fluxes as measured (blue bars) and with five-year moving average (yellow line). The 5-year moving average of FOSA flux to Devon Ice Cap from Pickard et al.[1] is superimposed for comparison (red line).

## 4.0 Evidence of indirect sources of PFAAs on Mt. Oxford icefield

**Table S14:** Pearson's correlation (r) matrix, and associated p-value for PFAS homologues. Weak correlations (r = 0.3-0.5) are shown in blue, moderate correlations (r= 0.5-0.7) shown in green, strong correlations (r= 0.7-0.9) are shown in red, and very strong correlations (0.9-1.0) are shown in purple. Statistically significant p-values (p<0.05) are also highlighted in bold. Data for C2-C4 PFCAs from Pickard et al.[3]

| | | TFA | PFPrA | PFBA | PFPeA | PFHxA | PFHpA | PFOA | PFNA | PFDA | PFUnDA | PFDoDA | PFBS | PFOS | PFECHS |
|---|---|---|---|---|---|---|---|---|---|---|---|---|---|---|---|
| **TFA** | r | | 0.77 | 0.91 | 0.64 | 0.83 | 0.84 | 0.76 | 0.80 | 0.75 | 0.73 | 0.48 | -0.10 | -0.12 | -0.08 |
| | p | | 1.E-14 | 1.E-14 | 5.E-6 | 3.E-13 | 1E-13 | 5E-10 | 2.E-11 | 3.E-09 | 1.E-06 | 0.02 | 0.50 | 0.41 | 0.60 |
| **PFPrA** | r | 0.77 | | 0.77 | 0.58 | 0.70 | 0.77 | 0.70 | 0.75 | 0.71 | 0.60 | 0.60 | -0.16 | -0.09 | 0.05 |
| | p | 1.E-14 | | 1.E-14 | 4.E-05 | 2.E-08 | 1.E-10 | 1.E-08 | 9.E-10 | 2.E-06 | 2.E-04 | 3.E-03 | 0.30 | 0.54 | 0.71 |
| **PFBA** | r | 0.91 | 0.70 | | 0.74 | 0.75 | 0.73 | 0.53 | 0.69 | 0.64 | 0.58 | 0.42 | 0.08 | -0.15 | 0.04 |
| | p | 1.E-14 | 3.E-06 | | 1.E-06 | 4.E-07 | 7.E-7 | 0.001 | 7.E-06 | 5.E-5 | 8.E-04 | 0.07 | 0.66 | 0.40 | 0.78 |
| **PFPeA** | r | 0.64 | 0.58 | 0.74 | | 0.66 | 0.78 | 0.70 | 0.79 | 0.82 | 0.71 | 0.56 | -0.30 | -0.02 | **-0.32** |
| | p | 5.E-6 | 4.E-05 | 1.E-06 | | 1.E-06 | 5.E-10 | 2.E-07 | 1.E-09 | 7.E-12 | 4.E-06 | 0.007 | 0.06 | 0.88 | **0.04** |
| **PFHxA** | r | 0.83 | 0.70 | 0.75 | 0.66 | | 0.90 | 0.77 | 0.82 | 0.75 | 0.77 | 0.72 | 0.10 | 0.03 | -0.02 |
| | p | 3.E-13 | 2.E-08 | 4.E-07 | 1.E-06 | | 2.E-18 | 1.E-10 | 2.E-12 | 1.E-09 | 1.E-07 | 4.E-06 | 0.50 | 0.83 | 0.84 |
| **PFHpA** | r | 0.84 | 0.77 | 0.73 | 0.78 | 0.90 | | 0.87 | 0.96 | 0.90 | 0.80 | 0.60 | -0.11 | -0.13 | -0.04 |
| | p | 1E-13 | 1.E-10 | 7.E-7 | 5.E-10 | 2.E-18 | | 6.E-16 | 5.E-27 | 1.E-18 | 2.E-08 | 0.003 | 0.45 | 0.37 | 0.76 |
| **PFOA** | r | 0.76 | 0.70 | 0.53 | 0.70 | 0.77 | 0.87 | | 0.90 | 0.87 | 0.68 | 0.53 | -0.19 | -0.13 | 0.03 |
| | p | 5E-10 | 1.E-08 | 0.001 | 2.E-07 | 1.E-10 | 6.E-16 | | 6.E-19 | 1.E-15 | 1.E-05 | 0.010 | 0.20 | 0.40 | 0.83 |
| **PFNA** | r | 0.80 | 0.75 | 0.69 | 0.79 | 0.82 | 0.96 | 0.90 | | 0.94 | 0.87 | 0.63 | -0.21 | -0.15 | -0.19 |
| | p | 2.E-11 | 9.E-10 | 7.E-06 | 1.E-09 | 2.E-12 | 5.E-27 | 6.E-19 | | 2.E-22 | 4.E-11 | 0.001 | 0.17 | 0.31 | 0.20 |
| **PFDA** | r | 0.75 | 0.71 | 0.64 | 0.80 | 0.75 | 0.90 | 0.87 | 0.94 | | 0.93 | 0.76 | -0.23 | -0.18 | -0.07 |
| | p | 3.E-09 | 2.E-06 | 5.E-5 | 9.E-10 | 1.E-09 | 1.E-18 | 1.E-15 | 2.E-22 | | 1.E-15 | 3.E-05 | 0.11 | 0.25 | 0.62 |
| **PFUnDA** | r | 0.73 | 0.60 | 0.58 | 0.71 | 0.77 | 0.80 | 0.68 | 0.87 | 0.93 | | 0.69 | -0.04 | 0.02 | 0.03 |
| | p | 1.E-06 | 2.E-04 | 8.E-04 | 4.E-06 | 1.E-07 | 2.E-08 | 1.E-05 | 4.E-11 | 1.E-15 | | 1.E-03 | 0.81 | 0.90 | 0.83 |
| **PFDoDA** | r | 0.48 | 0.60 | 0.42 | 0.56 | 0.72 | 0.60 | 0.53 | 0.63 | 0.76 | 0.69 | | **-0.46** | -0.37 | -0.30 |
| | p | 0.02 | 3.E-03 | 0.07 | 0.007 | 4.E-06 | 0.003 | 0.010 | 0.001 | 3.E-05 | 1.E-03 | | **0.04** | 0.10 | 0.09 |
| **PFBS** | r | -0.10 | -0.16 | 0.08 | -0.30 | 0.10 | -0.11 | -0.19 | -0.21 | -0.23 | -0.04 | -0.46 | | 0.90 | 0.23 |
| | p | 0.50 | 0.30 | 0.66 | 0.06 | 0.50 | 0.45 | 0.20 | 0.17 | 0.11 | 0.81 | 0.04 | | 2.E-16 | 0.30 |
| **PFOS** | r | -0.12 | -0.09 | -0.15 | -0.02 | 0.03 | -0.13 | -0.13 | -0.15 | -0.18 | 0.02 | -0.37 | 0.90 | | 0.06 |
| | p | 0.41 | 0.54 | 0.399 | 0.88 | 0.83 | 0.37 | 0.40 | 0.31 | 0.25 | 0.90 | 0.10 | 2.E-16 | | 0.66 |
| **PFECHS** | r | -0.08 | 0.05 | 0.04 | -0.32 | -0.02 | -0.04 | 0.03 | -0.19 | -0.07 | -0.30 | 0.23 | 0.06 | 0.07 | |
| | p | 0.60 | 0.71 | 0.78 | 0.04 | 0.84 | 0.76 | 0.83 | 0.20 | 0.62 | 0.09 | 0.30 | 0.66 | 0.61 | |
| **FOSA** | r | -9.E-03 | 0.11 | -0.29 | 0.38 | 0.40 | 0.42 | 0.40 | 0.46 | 0.34 | 0.14 | 0.06 | -0.17 | 0.19 | -0.18 |
| | p | 0.96 | 0.53 | 0.13 | 0.03 | 0.03 | 0.02 | 0.02 | 0.01 | 0.05 | 0.47 | 0.82 | 0.41 | 0.35 | 0.37 |

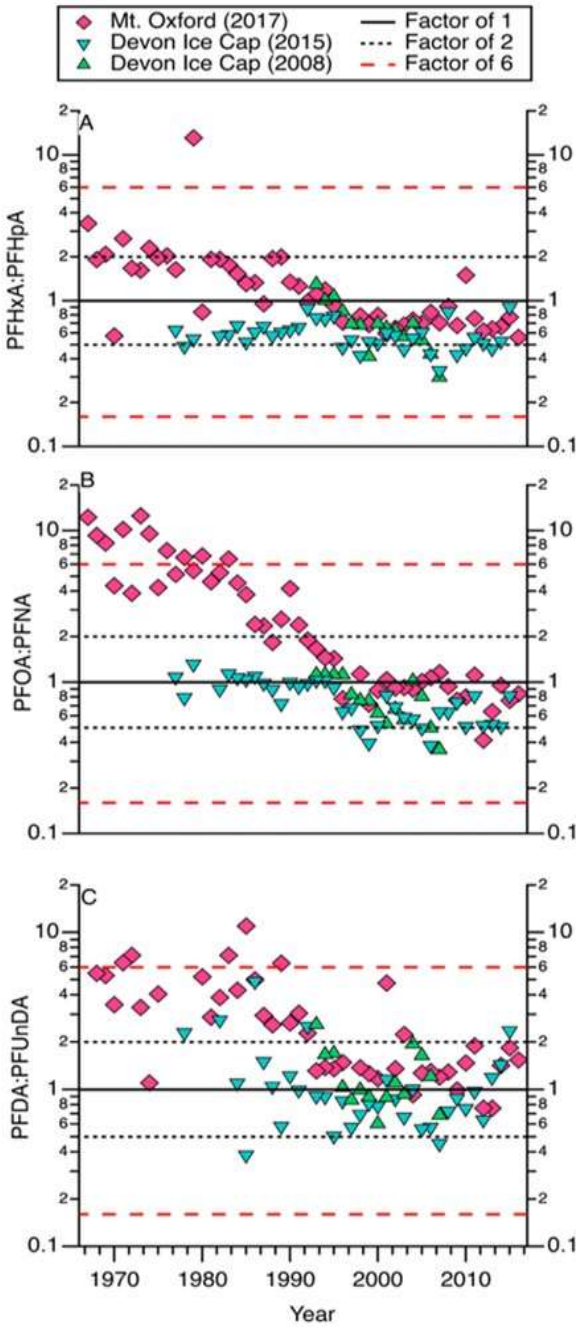


**Figure S5:** Molar flux ratios of even-odd PFCA pairs: (A) PFHxA:PFHpA, (B) PFOA:PFNA and (C) PFDA:PFUnDA as a function of time. The ratios of previous studies at the Devon Ice cap (2015 and 2008) are also included for comparison. The solid black line represents molar flux ratio corresponding to 1 (i.e., equal molar amounts are deposited), whereas dashed black and red lines correspond to molar flux ratios within a factor of ± 2 and ± 6, respectively.

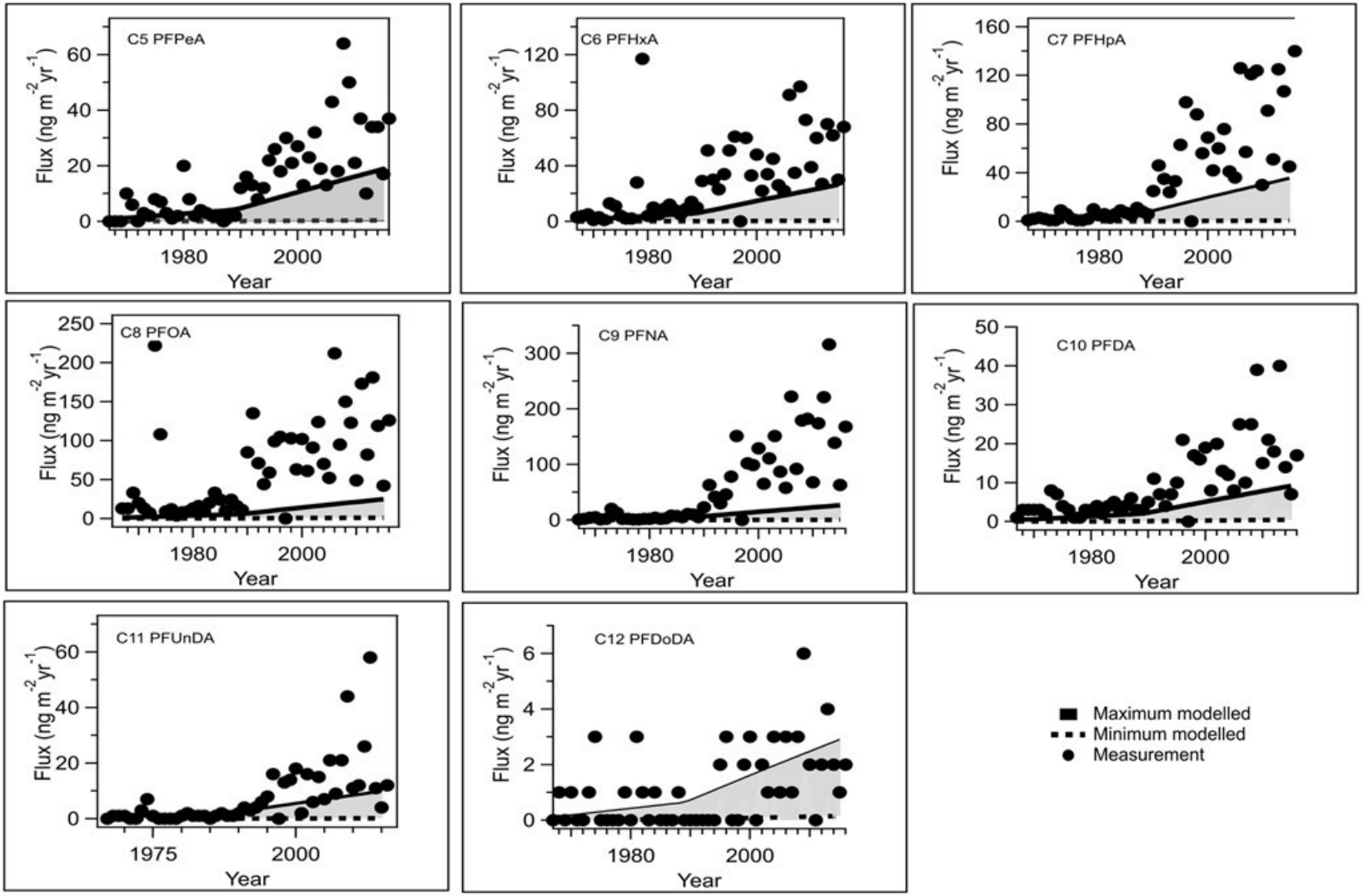


**Figure S6:** Measured (symbols) and modeled comparisons of C5 – C12 PFCAs to the Mt. Oxford icefield over the years 1967 – 2016. The modeled maximum (black line) and minimum (broken line) are from Thackray et al.[18]

## 5.0 Evidence for aerosol transport of PFAAs

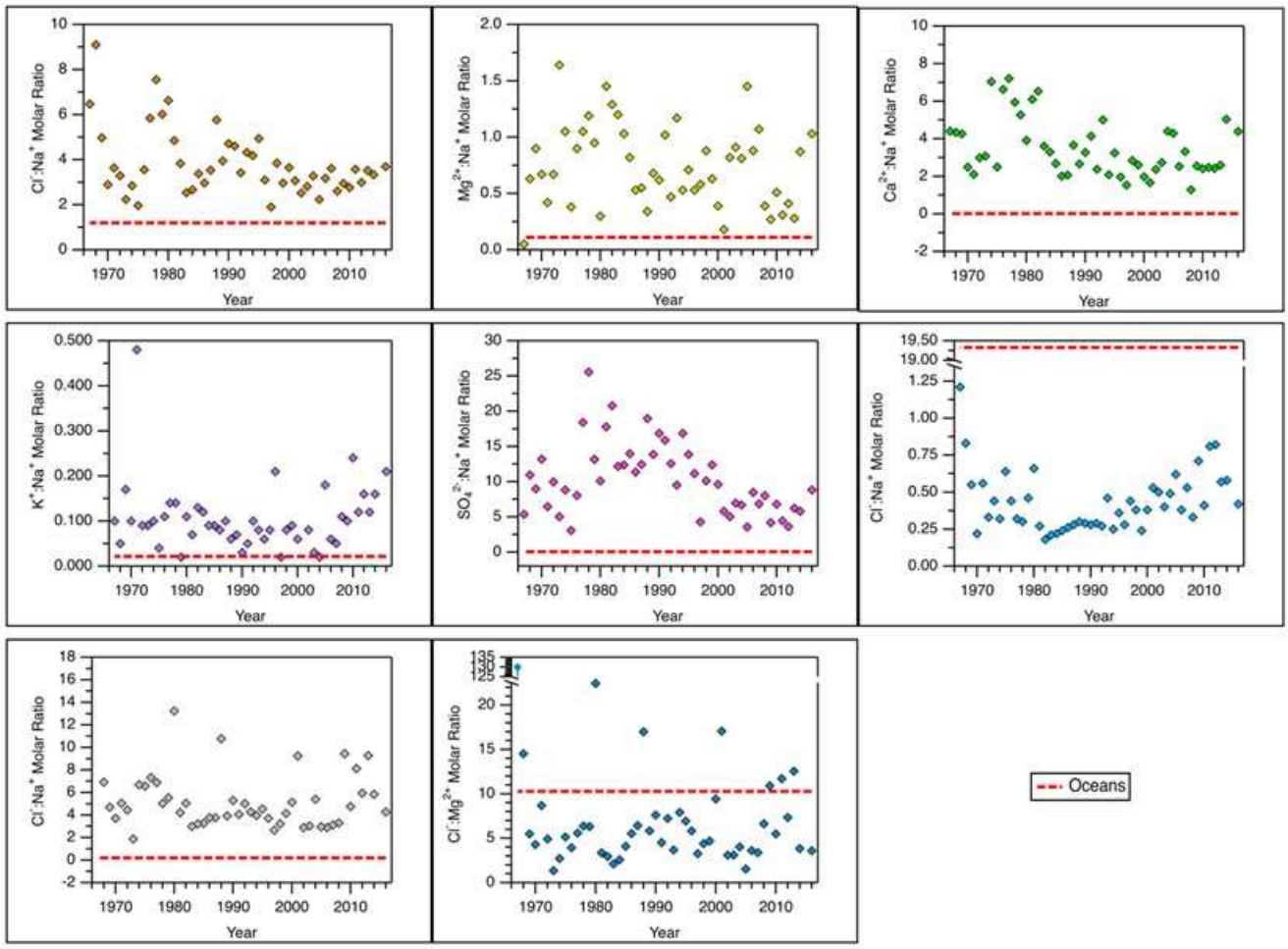


**Figure S7:** Calculated molar ratios of major ions (y-axis) as a function of time from Mt. Oxford icefield (1967 – 2016). Molar ratio typical of bulk seawater is represented by the dashed red line.

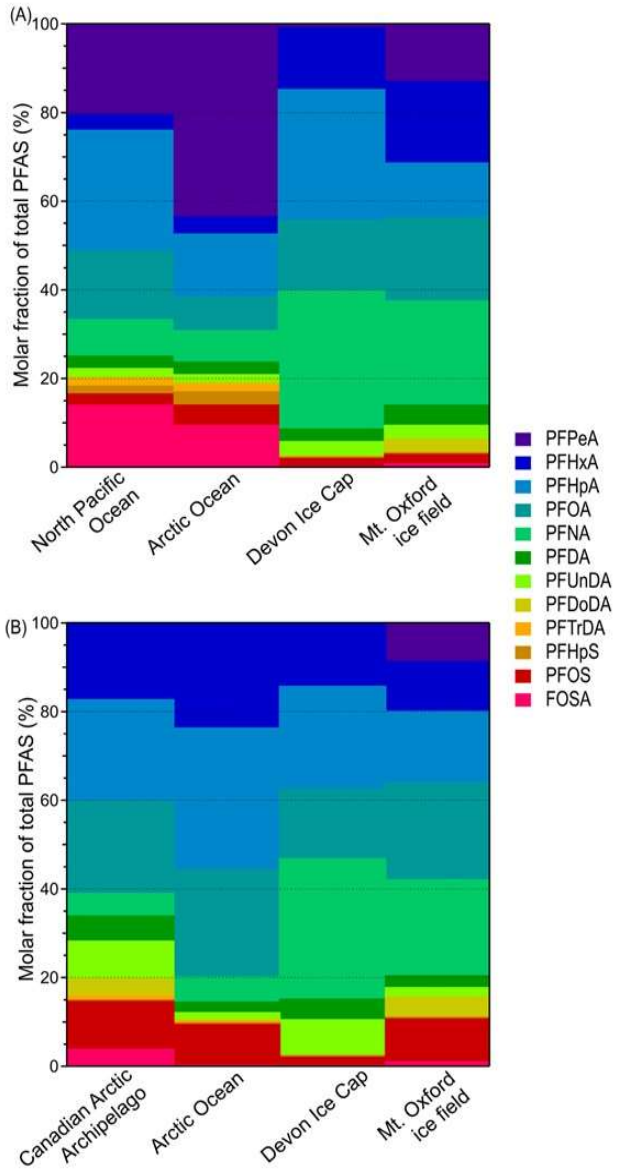


**Figure S8:** Molar concentration fraction of selected PFAAs on the Mt. Oxford icefield compared to levels in the Canadian Arctic Archipelago,[19] Arctic Ocean,[19,20] North Atlantic Ocean[21] and North Pacific Ocean[20] in (A) 2010 and (B) 2005.

**Table S15:** Depth profile (cm) of cations (ng $mL^{-1}$) on Mt. Oxford icefield. Values <LOD are identified in red. Due to insufficient volume of sample available for analysis, the year 2015 do not have concentration values. Lithium was <0.0087 for all samples analyzed.

| LOD (ng $mL^{-1}$) | | 0.0013 | 0.00035 | 0.01282 | 0.05107 | 0.06377 |
|---|---|---|---|---|---|---|
| **Depth** | **Year** | **Sodium** | **Ammonium** | **Potassium** | **Magnesium** | **Calcium** |
| 41 | 2016 | 23.28 | 13.70 | 8.13 | 25.28 | 181.14 |
| 89 | 2014 | 19.88 | 2.50 | 5.27 | 18.18 | 177.85 |
| 138 | 2013 | 15.59 | 4.19 | 3.12 | 4.62 | 71.97 |
| 163 | 2012 | 20.06 | <0.00035 | 5.49 | 8.64 | 86.09 |
| 191 | 2011 | 17.73 | <0.00035 | 3.62 | 5.74 | 78.19 |
| 227 | 2010 | 24.92 | 24.37 | 10.11 | 13.32 | 106.49 |
| 279 | 2009 | 24.78 | 0.61 | 4.00 | 7.08 | 112.34 |
| 325 | 2008 | 31.03 | 4.61 | 5.88 | 12.87 | 71.09 |
| 353 | 2007 | 12.66 | 0.00 | 1.03 | 14.32 | 74.63 |
| 399 | 2006 | 17.48 | 10.09 | 1.91 | 16.20 | 78.61 |
| 413 | 2005 | 19.31 | 19.78 | 5.93 | 29.63 | 146.89 |
| 447 | 2004 | 15.73 | <0.00035 | 0.48 | 13.55 | 122.82 |
| 490 | 2003 | 16.55 | <0.00035 | 0.76 | 15.86 | 80.53 |
| 517 | 2002 | 22.49 | 30.13 | 3.07 | 19.45 | 94.43 |
| 545 | 2001 | 14.52 | 0.03 | < 0.01282 | 2.75 | 42.75 |
| 587 | 2000 | 16.48 | 16.03 | 1.58 | 6.74 | 58.01 |
| 615 | 1999 | 17.48 | 35.81 | 2.63 | 11.68 | 81.07 |
| 661 | 1998 | 16.27 | 30.66 | 2.08 | 15.12 | 82.09 |
| 687 | 1997 | 39.26 | 10.18 | 1.64 | 24.11 | 107.24 |
| 733 | 1996 | 19.77 | 15.65 | 7.20 | 11.12 | 69.28 |
| 775 | 1995 | 11.69 | 22.03 | 1.58 | 8.81 | 67.16 |
| 809 | 1994 | 15.09 | 56.88 | 1.58 | 8.43 | 56.08 |
| 835 | 1993 | 13.37 | 16.97 | 1.86 | 16.61 | 118.88 |
| 878 | 1992 | 18.09 | 31.00 | 2.96 | 9.06 | 76.28 |
| 920 | 1991 | 11.08 | 23.00 | 1.03 | 11.97 | 81.48 |
| 971 | 1990 | 9.98 | 37.39 | 0.42 | 6.52 | 57.99 |
| 987 | 1989 | 15.16 | 13.11 | 1.86 | 10.89 | 71.61 |
| 1010 | 1988 | 6.76 | 13.70 | 0.65 | 2.43 | 43.88 |
| 1057 | 1987 | 18.88 | 9.35 | 3.18 | 10.99 | 69.45 |
| 1079 | 1986 | 19.31 | 8.16 | 2.52 | 10.91 | 68.95 |
| 1103 | 1985 | 16.16 | 14.17 | 2.41 | 14.07 | 76.99 |
| 1138 | 1984 | 20.42 | 18.37 | 2.96 | 22.20 | 119.59 |
| 1172 | 1983 | 26.10 | 17.23 | 5.49 | 33.17 | 167.25 |
| 1190 | 1982 | 11.30 | 34.41 | 2.41 | 15.43 | 130.90 |
| 1233 | 1981 | 14.34 | 21.26 | 1.80 | 21.94 | 155.20 |
| 1277 | 1980 | 9.44 | 13.61 | 1.69 | 2.95 | 65.47 |
| 1300 | 1979 | 9.69 | 10.45 | 0.31 | 9.76 | 90.79 |
| 1318 | 1978 | 7.26 | 19.49 | 1.69 | 9.10 | 76.67 |
| 1332 | 1977 | 7.72 | 21.64 | 1.86 | 8.56 | 98.89 |
| 1363 | 1976 | 12.12 | 10.61 | 2.19 | 11.58 | 142.52 |
| 1389 | 1975 | 24.99 | 13.33 | 1.80 | 10.05 | 110.82 |
| 1410 | 1974 | 17.77 | 21.22 | 3.12 | 19.76 | 221.94 |
| 1438 | 1973 | 27.17 | 12.93 | 4.17 | 47.14 | 148.35 |
| 1461 | 1972 | 12.41 | 8.83 | 1.86 | 8.80 | 65.62 |
| 1482 | 1971 | 15.70 | 18.98 | 12.81 | 6.93 | 58.68 |
| 1515 | 1970 | 15.16 | 16.21 | 2.68 | 10.74 | 66.91 |
| 1547 | 1969 | 9.40 | 33.63 | 2.68 | 8.99 | 71.03 |
| 1575 | 1968 | 6.19 | 30.09 | 0.48 | 4.10 | 47.54 |
| 1588 | 1967 | 6.65 | 0.41 | 1.09 | 0.35 | 51.93 |

**Table S16**:Depth profile (cm) of anions (ng $mL^{-1}$) detected on Mt. Oxford icefield. Due to insufficient volume of sample available for analysis, the year 2015 do not have concentration values. Bromide and Nitrite was <LOD for all samples analyzed.

| LOD (ng $mL^{-1}$) | | 0.22 | 1.93 | 5.70 | 11.90 | 23.49 |
|---|---|---|---|---|---|---|
| **Depth** | **Year** | **Fluoride** | **Chloride** | **Sulfate** | **Phosphate** | **Nitrate** |
| 41 | 2016 | 435.39 | 132.36 | 855.52 | 150.63 | 342.96 |
| 89 | 2014 | 56.08 | 102.04 | 479.53 | 150.74 | 405.73 |
| 138 | 2013 | 244.78 | 84.66 | 404.28 | 134.91 | 345.53 |
| 163 | 2012 | 241.63 | 92.34 | 303.89 | 153.25 | 129.45 |
| 191 | 2011 | 151.42 | 97.88 | 328.20 | 125.42 | 361.83 |
| 227 | 2010 | 326.08 | 106.48 | 708.00 | 111.56 | 550.02 |
| 279 | 2009 | 252.68 | 112.70 | 433.03 | 145.39 | 243.71 |
| 325 | 2008 | 295.14 | 124.51 | 1036.44 | 106.43 | 382.28 |
| 353 | 2007 | 348.49 | 70.48 | 362.86 | 102.18 | 177.22 |
| 399 | 2006 | 339.18 | 85.51 | 617.75 | 107.31 | 424.90 |
| 413 | 2005 | 142.50 | 66.32 | 288.25 | 94.43 | 297.20 |
| 447 | 2004 | 401.37 | 79.47 | 440.00 | 116.14 | 182.37 |
| 490 | 2003 | 273.51 | 71.65 | 479.53 | 108.94 | 119.44 |
| 517 | 2002 | 400.90 | 87.25 | 472.97 | 99.34 | 365.69 |
| 545 | 2001 | 353.94 | 68.52 | 351.45 | 106.65 | 90.42 |
| 587 | 2000 | 254.65 | 92.66 | 662.56 | 113.31 | 446.77 |
| 615 | 1999 | 245.49 | 79.90 | 905.61 | 180.96 | 427.76 |
| 661 | 1998 | 331.44 | 96.60 | 687.71 | 114.40 | 395.15 |
| 687 | 1997 | 99.72 | 114.94 | 702.08 | 119.53 | 205.82 |
| 733 | 1996 | 309.58 | 94.58 | 921.25 | 192.10 | 441.05 |
| 775 | 1995 | 29.24 | 89.03 | 676.51 | 108.40 | 469.94 |
| 809 | 1994 | 452.12 | 97.21 | 1062.44 | 94.87 | 418.75 |
| 835 | 1993 | 446.12 | 89.17 | 530.67 | 168.31 | 404.30 |
| 878 | 1992 | 124.58 | 95.50 | 949.79 | 114.83 | 503.83 |
| 920 | 1991 | 196.80 | 78.62 | 735.26 | 110.58 | 162.92 |
| 971 | 1990 | 220.00 | 72.43 | 702.29 | 140.70 | 100.00 |
| 987 | 1989 | 243.36 | 92.44 | 878.14 | 114.18 | 394.87 |
| 1010 | 1988 | 295.69 | 60.10 | 535.75 | 112.65 | 284.47 |
| 1057 | 1987 | 365.46 | 102.89 | 981.70 | 132.08 | 365.41 |
| 1079 | 1986 | 306.74 | 88.21 | 914.70 | 121.06 | 176.36 |
| 1103 | 1985 | 336.57 | 84.16 | 942.81 | 175.07 | 348.68 |
| 1138 | 1984 | 200.90 | 83.98 | 1055.04 | 98.47 | 338.24 |
| 1172 | 1983 | 311.08 | 102.01 | 1329.80 | 98.47 | 425.32 |
| 1190 | 1982 | 130.12 | 66.71 | 980.64 | 147.46 | 516.85 |
| 1233 | 1981 | 583.60 | 107.34 | 1064.97 | 128.48 | 488.10 |
| 1277 | 1980 | 219.61 | 96.35 | 397.52 | 144.41 | 262.87 |
| 1300 | 1979 | 255.75 | 89.99 | 532.36 | 127.60 | 154.62 |
| 1318 | 1978 | 244.07 | 84.55 | 775.63 | 112.43 | 185.80 |
| 1332 | 1977 | 273.67 | 69.55 | 593.87 | 122.47 | 280.89 |
| 1363 | 1976 | 362.30 | 66.53 | 406.19 | 115.16 | 170.93 |
| 1389 | 1975 | 354.96 | 75.35 | 321.43 | 130.00 | 85.41 |
| 1410 | 1974 | 345.02 | 77.98 | 653.47 | 130.88 | 88.99 |
| 1438 | 1973 | 473.11 | 93.48 | 571.89 | 118.33 | 176.36 |
| 1461 | 1972 | 410.37 | 62.94 | 515.67 | 110.47 | 252.86 |
| 1482 | 1971 | 33.98 | 87.86 | 423.10 | 124.55 | 94.28 |
| 1515 | 1970 | 283.06 | 67.49 | 834.60 | 110.58 | 359.11 |
| 1547 | 1969 | 241.00 | 72.01 | 352.50 | 107.85 | 233.27 |
| 1575 | 1968 | 361.99 | 86.79 | 282.55 | 122.04 | 269.45 |
| 1588 | 1967 | 410.62 | 66.32 | 148.67 | 136.32 | 102.16 |

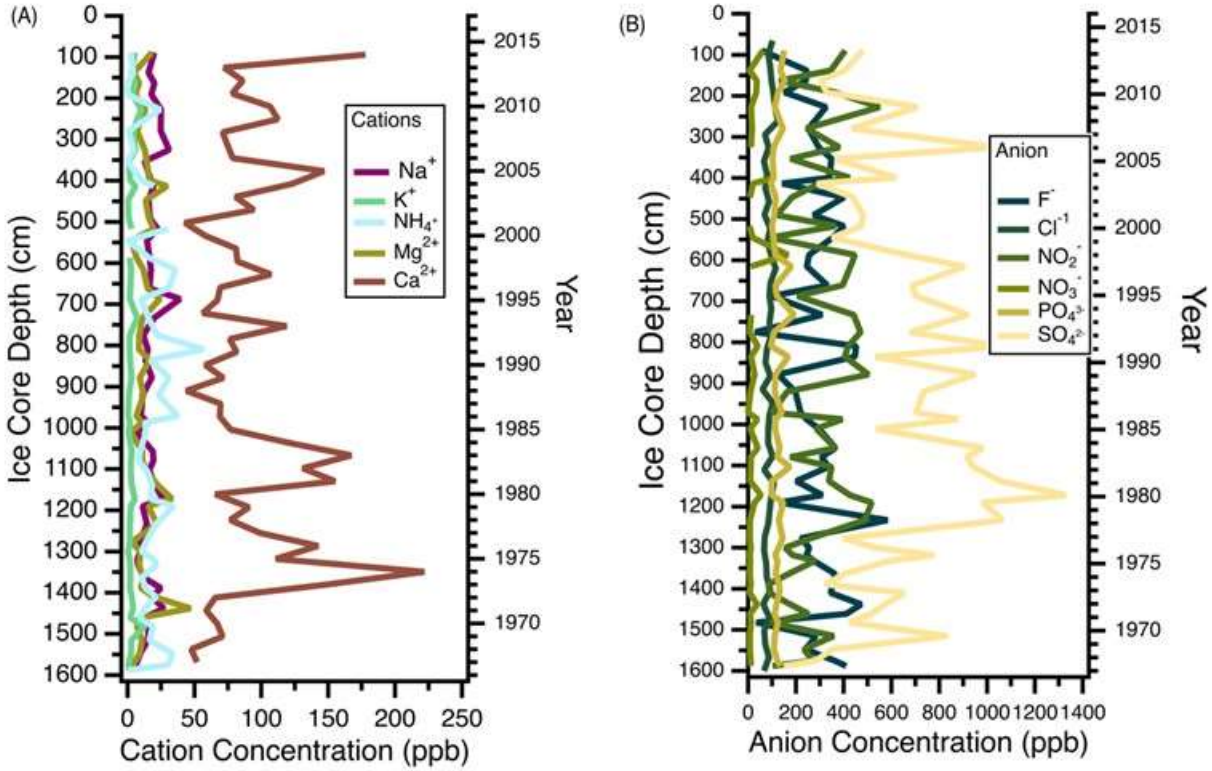


**Figure S9:** Depth profiles of (A) cation and (B) anion concentrations (ng $mL^{-1}$) on Mt Oxford icefield.

To understand the contribution of sea salt and non-sea salt aerosols to the Mt. Oxford icefield, we calculated the contribution of each anion and cation that are commonly found in marine aerosols. Table S17 is a summary of our findings. To calculate the nss-component, we first determined the average molar concentration of the ions in the core from 1967 – 2016. We then subtracted the individual ion molar concentration from the sodium molar concentration and multiplied this value by the expected ion to sodium ratio, taken from Libes, 2009.[22] Finally, the sea salt concentration and the percentage of non – sea salt were determined by taking the difference between the total average concentration and the average non-sea salt concentration.

The PFAAs detected were correlated with the cations and anions to determine if there were any statistically significant correlations. Ions were converted to flux as described earlier.

**Table S17:** Non-sea salt and sea salt component concentrations (µmol/L) of selected ions in the ice core.

| | $Na^+$ | $K^+$ | $Mg^{2+}$ | $Ca^{2+}$ | $Cl^-$ | $SO_4^{2-}$ | $F^-$ |
|---|---|---|---|---|---|---|---|
| **Average molar conc. in the ice core (µmol/L)** | 0.723 | 0.076 | 0.536 | 2.302 | 2.457 | 6.712 | 15.056 |
| **Average non – sea salt conc. (µmol/L)** | | 0.060 | 0.450 | 2.240 | 1.590 | 6.530 | 14.750 |
| **Sea salt conc. (µmol/L)** | | 0.016 | 0.086 | 0.062 | 0.867 | 0.182 | 0.306 |
| **Contribution of non – sea salt component** | | 77.63 | 83.11 | 97.33 | 64.68 | 97.36 | 98.00 |

**Table S18:** Pearson's correlation coefficient (r) and associated p-value, including data points (n) of PFAA homologues with measured cations for the period 1967 – 2016 and 1967 – 1979. Weak correlations (r = 0.3-0.5) are shown in green, moderate correlations (r = 0.5-0.7) are shown in blue, and strong correlations (r = 0.7-1.0) are shown in red. Statistically significant p-values (p<0.05) are highlighted in bold. Cases where a Pearson correlation could not be calculated due to insufficient sample size are indicated by (-)

| | | 1967 – 2016 | | | | | | | 1967-1979 | | |
|---|---|---|---|---|---|---|---|---|---|---|---|
| | | $Na^+$ | nss-$K^+$ | nss-$Mg^{2+}$ | nss-$Ca^{2+}$ | nss-$Cl^-$ | nss-$SO_4^{2-}$ | $PO_4^{3-}$ | $Na^+$ | nss-$Mg^{2+}$ | nss-$Ca^{2+}$ |
| **TFA** | r | 0.28 | **0.30** | 0.15 | 0.17 | 0.19 | 0.06 | 0.04 | | | |
| | p | 0.06 | **0.04** | 0.33 | 0.25 | 0.19 | 0.68 | 0.80 | | | |
| | n | 47 | **46** | 46 | 47 | 47 | 47 | 47 | | | |
| **PFPrA** | r | **0.46** | **0.36** | 0.17 | 0.28 | **0.32** | 0.28 | 0.12 | | | |
| | p | **0.0001** | **0.01** | 0.26 | 0.05 | **0.03** | 0.05 | 0.42 | | | |
| | n | **49** | **48** | 48 | 49 | **49** | 49 | 49 | | | |
| **PFBA** | R | 0.29 | **0.38** | -0.20 | 0.19 | 0.22 | 0.03 | 0.13 | -0.08 | | 0.05 |
| | p | 0.10 | **0.03** | 0.27 | 0.28 | 0.21 | 0.89 | 0.45 | 0.95 | | 0.97 |
| | n | 34 | **33** | 33 | 34 | 34 | 34 | 34 | 3 | | 3 |
| **PFPeA** | r | **0.42** | 0.30 | 0.002 | 0.11 | **0.36** | 0.01 | 0.23 | **0.54** | -0.05 | 0.03 |
| | p | **0.01** | 0.06 | 0.99 | 0.48 | **0.02** | 0.93 | 0.14 | **0.17** | 0.91 | 0.95 |
| | n | **43** | 42 | 43 | 43 | **43** | 43 | 43 | **8** | 8 | 8 |
| **PFHxA** | r | **0.35** | 0.10 | 0.12 | 0.14 | 0.29 | 0.21 | 0.13 | 0.02 | 0.27 | 0.20 |
| | p | **0.02** | 0.49 | 0.42 | 0.35 | 0.05 | 0.16 | 0.37 | 0.95 | 0.42 | 0.54 |
| | n | **47** | 46 | 46 | 47 | 47 | 47 | 47 | 12 | 11 | 12 |
| **PFHpA** | r | **0.41** | 0.21 | 0.07 | 0.14 | 0.28 | 0.14 | 0.14 | **0.38** | **0.60** | **0.55** |
| | p | **0.0053** | 0.15 | 0.65 | 0.35 | 0.06 | 0.36 | 0.34 | **0.21** | **0.04** | **0.05** |
| | n | **48** | 47 | 47 | 48 | 48 | 0 | 48 | **13** | **12** | **13** |
| **PFOA** | r | **0.49** | **0.32** | 0.24 | 0.25 | **0.31** | 0.13 | 0.19 | **0.56** | **0.84** | **0.59** |
| | p | **0.0004** | **0.03** | 0.11 | 0.01 | **0.03** | 0.38 | 0.18 | **0.05** | **0.0007** | **0.03** |
| | n | **48** | **47** | 47 | 48 | **48** | 48 | 48 | **13** | **12** | **13** |
| **PFNA** | r | **0.36** | 0.24 | 0.01 | 0.06 | 0.14 | 0.03 | 0.03 | **0.66** | **0.88** | **0.71** |
| | p | **0.01** | 0.10 | 0.96 | 0.71 | 0.35 | 0.54 | 0.84 | **0.02** | **0.0003** | **0.01** |
| | n | **47** | 46 | 46 | 47 | 47 | 47 | 47 | **12** | **11** | **12** |
| **PFDA** | r | **0.45** | **0.32** | 0.05 | 0.13 | 0.23 | -0.03 | 0.11 | **0.70** | **0.73** | **0.76** |
| | p | **0.001** | **0.03** | 0.72 | 0.40 | 0.12 | 0.86 | 0.46 | **0.02** | **0.01** | **0.01** |
| | n | **46** | **45** | 46 | 46 | 46 | 46 | 46 | **11** | **11** | **11** |
| **PFUnDA** | r | 0.11 | 0.28 | -0.08 | -0.06 | 0.04 | -0.17 | -0.02 | -0.76 | **0.39** | **0.99** |
| | p | 0.54 | 0.12 | 0.65 | 0.00 | 0.82 | 0.35 | 0.90 | 0.45 | 0.74 | 0.09 |
| | n | 32 | 31 | 32 | 32 | 32 | 32 | 32 | 3 | 3 | 3 |
| **PFDoDA** | r | **0.52** | 0.36 | -0.19 | 0.24 | 0.38 | 0.17 | 0.39 | 0.25 | **0.33** | **0.81** |
| | p | **0.02** | 0.10 | 0.41 | 0.27 | 0.08 | 0.45 | 0.07 | 0.69 | 0.58 | 0.09 |
| | n | **22** | 22 | 22 | 22 | 22 | 22 | 22 | 5 | 5 | 5 |
| **PFOS** | r | 0.03 | -0.06 | -0.24 | 0.11 | -0.03 | 0.13 | -0.05 | **0.32** | **0.48** | **0.49** |
| | p | 0.83 | 0.70 | 0.12 | 0.48 | 0.85 | 0.39 | 0.74 | 0.32 | 0.31 | 0.11 |
| | n | 43 | 43 | 42 | 43 | 43 | 43 | 43 | 12 | 11 | 12 |
| **PFBS** | r | 0.03 | -0.18 | 0.14 | 0.07 | -0.04 | 0.08 | -0.09 | **0.34** | 0.27 | **0.42** |
| | p | 0.84 | 0.25 | 0.37 | 0.64 | 0.80 | 0.63 | 0.57 | 0.27 | 0.07 | 0.17 |
| | n | 42 | 42 | 41 | 43 | 42 | 42 | 42 | 12 | 0 | 12 |
| **PFECHS** | r | **0.52** | 0.29 | 0.18 | **0.49** | **0.59** | **0.42** | **0.56** | **0.72** | **0.55** | **0.54** |
| | p | **0.0001** | 0.05 | 0.25 | **0.0005** | **1.6E-5** | **0.003** | **0.0001** | **0.01** | 0.06 | **0.05** |
| | n | **46** | 46 | 45 | **46** | **46** | **46** | **46** | **12** | 12 | **13** |
| **FOSA** | r | -0.04 | -0.21 | -0.04 | -0.25 | -0.05 | -0.09 | -0.08 | | | |
| | p | 0.83 | 0.28 | 0.82 | 0.18 | 0.77 | 0.64 | 0.68 | | | |
| | n | 30 | 0 | 30 | 30 | 30 | 30 | 30 | | | |

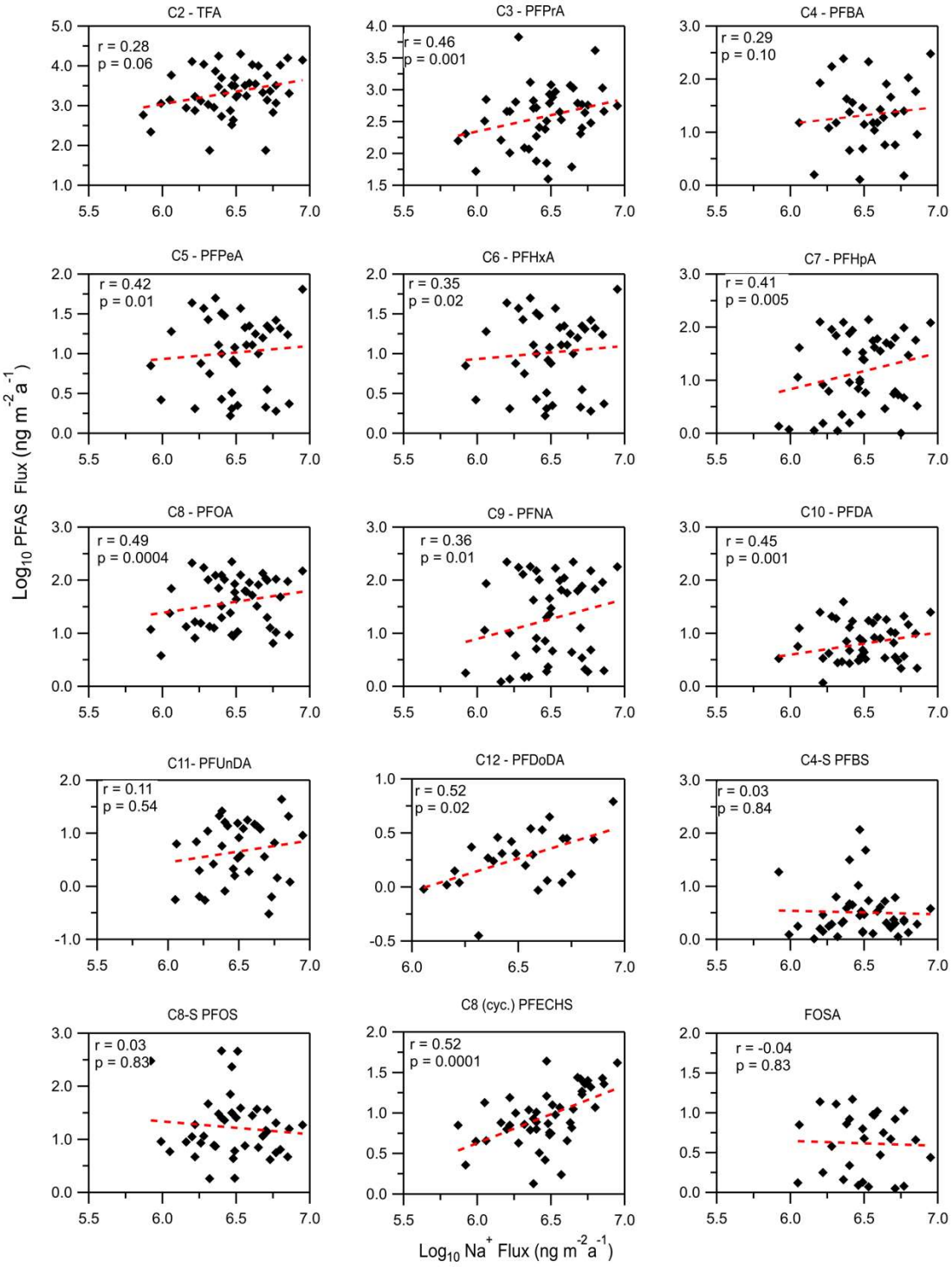


**Figure S10:** Correlation between log-transformed fluxes of $Na^+$ and C2 – C12 PFCAs, PFSAs (C4, C8, cyclic C8)) and FOSA. The dashed red line represents a line of best fit (y = mx + b), the Pearson correlation (r) and p-value is also included.

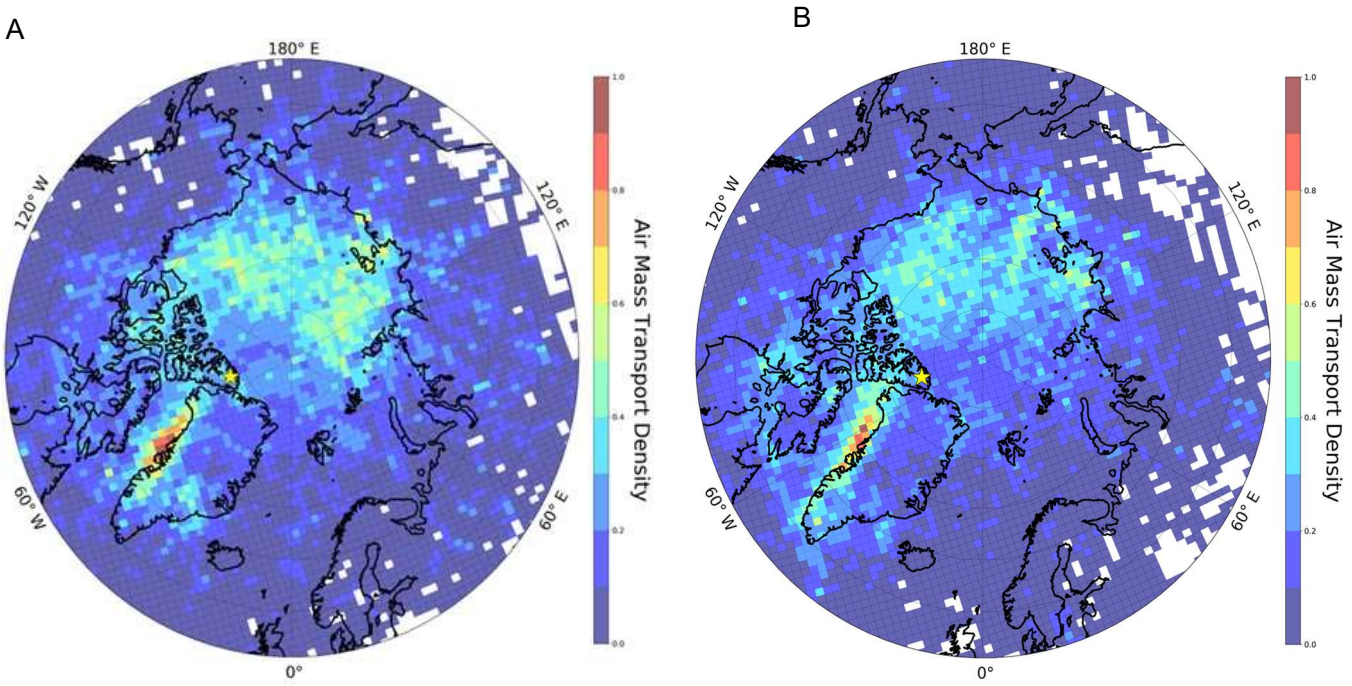


**Figure S11:** Air mass transport density map for air parcels arriving at Mt. Oxford, icefield (yellow star) for (A) 2001 and (B) 2013.

## References


(1) Criscitiello, A. S.; Das, S. B.; Karnauskas, K. B.; Evans, M. J.; Frey, K. E.; Joughin, I.; Steig, E. J.; McConnell, J. R.; Medley, B. Tropical Pacific Influence on the Source and Transport of Marine Aerosols to West Antarctica. *J. Clim.* **2014**, *27* (3), 1343–1363. https://doi.org/10.1175/JCLI-D-13-00148.1.

(2) McConnell, J. R.; Lamorey, G. W.; Lambert, S. W.; Taylor, K. C. Continuous Ice-Core Chemical Analyses Using Inductively Coupled Plasma Mass Spectrometry. *Environ. Sci. Technol.* **2002**, *36* (1), 7–11. https://doi.org/10.1021/es011088z.

(3) Draxler, R. R.; Hess, G. D. An Overview of the HYSPLIT_4 Modelling System for Trajectories, Dispersion and Deposition. *Aust. Meteorol. Mag.* **1998**, *47* (4), 295–308.

(4) Criscitiello, A. S.; Marshall, S. J.; Evans, M. J.; Kinnard, C.; Norman, A.-L.; Sharp, M. J. Marine Aerosol Source Regions to Prince of Wales Icefield, Ellesmere Island, and Influence from the Tropical Pacific, 1979–2001. *J. Geophys. Res. Atmos.* **2016**, *121* (16), 9492–9507. https://doi.org/https://doi.org/10.1002/2015JD024457.

(5) Criscitiello, A. S.; Geldsetzer, T.; Rhodes, R. H.; Arienzo, M.; McConnell, J.; Chellman, N.; Osman, M. B.; Yackel, J. J.; Marshall, S. Marine Aerosol Records of Arctic Sea-Ice and Polynya Variability From New Ellesmere and Devon Island Firn Cores, Nunavut, Canada. *J. Geophys. Res. Ocean.* **2021**, *126* (9), 1–20. https://doi.org/10.1029/2021JC017205.

(6) Stohl, A. Computation, Accuracy and Applications of Trajectories- a Review and Bibliography. *Atmospheic Environement* **1998**, *32* (6), 947–966. https://doi.org/10.1016/S1474-8177(02)80024-9.

(7) Dorling, S. R.; Davies, T. D. Extending Cluster Analysis-Synoptic Meteorology Links to Characterise Chemical Climates at Six Northwest European Monitoring Stations. *Atmos. Environ.* **1995**, *29* (2), 145–167. https://doi.org/10.1016/1352-2310(94)00251-F.

(8) Pickard, H. M.; Criscitiello, A. S.; Spencer, C.; Sharp, M. J.; Muir, D. C. G.; De Silva, A. O.; Young, C. J. Continuous Non-Marine Inputs of per- and Polyfluoroalkyl Substances to the High Arctic: A Multi-Decadal Temporal Record.

*Atmos. Chem. Phys.* **2018**, *18* (7), 5045–5058. https://doi.org/10.5194/acp-18-5045-2018.

(9) Macinnis, J. J.; French, K.; Muir, D. C. G.; Spencer, C.; Criscitiello, A.; De Silva, A. O.; Young, C. J. Emerging Investigator Series: A 14-Year Depositional Ice Record of Perfluoroalkyl Substances in the High Arctic. *Environ. Sci. Process. Impacts* **2017**, *19* (1), 22–30. https://doi.org/10.1039/c6em00593d.

(10) Young, C. J.; Furdui, V. I.; Franklin, J.; Koerner, R. M.; Muir, D. C. G.; Mabury, S. A. Perfluorinated Acids in Arctic Snow: New Evidence for Atmospheric Formation. *Environ. Sci. Technol.* **2007**, *41* (10), 3455–3461. https://doi.org/10.1021/es0626234.

(11) Wang, X.; Halsall, C.; Codling, G.; Xie, Z.; Xu, B.; Zhao, Z.; Xue, Y.; Ebinghaus, R.; Jones, K. C. Accumulation of Perfluoroalkyl Compunds in Tibetan Mountain Snow: Temporal Patterns from 1980 to 2010. *Environ. Sci. Technol.* **2014**, *48* (1), 173–181. https://doi.org/10.1021/es4044775.

(12) Kirchgeorg, T.; Dreyer, A.; Gabrieli, J.; Kehrwald, N.; Sigl, M.; Schwikowski, M.; Boutron, C.; Gambaro, A.; Barbante, C.; Ebinghaus, R. Temporal Variations of Perfluoroalkyl Substances and Polybrominated Diphenyl Ethers in Alpine Snow. *Environ. Pollut.* **2013**, *178* (3), 367–374. https://doi.org/10.1016/j.envpol.2013.03.043.

(13) Kwok, K. Y.; Taniyasu, S.; Yeung, L. W. Y.; Murphy, M. B.; Lam, P. K. S.; Horii, Y.; Kannan, K.; Petrick, G.; Sinha, R. K.; Yamashita, N. Flux of Perfluorinated Chemicals through Wet Deposition in Japan, the United States, and Several Other Countries. *Environ. Sci. Technol.* **2010**, *44* (18), 7043–7049. https://doi.org/10.1021/es101170c.

(14) Scott, B. F.; Spencer, C.; Mabury, S. A.; Muir, D. C. G. Poly and Perfluorinated Carboxylates in North American Precipitation. *Environ. Sci. Technol.* **2006**, *40* (23), 7167–7174.

(15) Plassmann, M. M.; Meyer, T.; Lei, Y. D.; Wania, F.; McLachlan, M. S.; Berger, U. Laboratory Studies on the Fate of Perfluoroalkyl Carboxylates and Sulfonates during Snowmelt. *Environ. Sci. Technol.* **2011**, *45* (16), 6872–6878. https://doi.org/10.1021/es201249d.

(16) Garnett, J.; Halsall, C.; Thomas, M.; Crabeck, O.; France, J.; Joerss, H.; Ebinghaus, R.; Kaiser, J.; Leeson, A.; Wynn, P. M. Investigating the Uptake and Fate of Poly- and Perfl Uoroalkylated Substances ( PFAS ) in Sea Ice Using an Experimental Sea Ice Chamber. *Environ. Sci. Technol.* **2021**.

(17) Moser, D. E.; Thomas, E. R.; Nehrbass-Ahles, C.; Eichler, A.; Wolff, E. Melt-Affected Ice Cores for (Sub-)Polar Research in a Warming World. *Egusph. Prepr.* **2023**, No. September, 1–48.

(18) Thackray, C. P.; Selin, N. E.; Young, C. J. A Global Atmospheric Chemistry Model for the Fate and Transport of PFCAs and Their Precursors. *Environ. Sci. Process. Impacts* **2019**, *22* (2), 285–293. https://doi.org/10.1039/c9em00326f.

(19) Benskin, J. P.; Muir, D. C. G.; Scott, B. F.; Spencer, C.; De Silva, A. O.; Kylin, H.; Martin, J. W.; Morris, A.; Lohmann, R.; Tomy, G.; Rosenberg, B.; Taniyasu, S.; Yamashita, N. Perfluoroalkyl Acids in the Atlantic and Canadian Arctic Oceans. *Environ. Sci. Technol.* **2012**, *46* (11), 5815–5823. https://doi.org/10.1021/es300578x.

(20) Cai, M. M.; Zhao, Z.; Yin, Z.; Ahrens, L.; Huang, P.; Cai, M. M.; Yang, H.; He, J.; Sturm, R.; Ebinghaus, R.; Xie, Z. Occurrence of Perfluoroalkyl Compounds in Surface Waters from the North Pacific to the Arctic Ocean. *Environ. Sci. Technol.* **2012**, *46* (2), 661–668. https://doi.org/10.1021/es2026278.

(21) Zhao, Z.; Xie, Z.; Möller, A.; Sturm, R.; Tang, J.; Zhang, G.; Ebinghaus, R. Distribution and Long-Range Transport of Polyfluoroalkyl Substances in the Arctic, Atlantic Ocean and Antarctic Coast. *Environ. Pollut.* **2012**, *170*, 71–77. https://doi.org/10.1016/j.envpol.2012.06.004.

(22) Libes, S. M. *Introduction to Marine Biogeochemistry*, 2nd ed.; Acedemic Press, 2009.